

Sołtan Institute for Nuclear Studies

**Single-particle effects in the properties  
of heavy and superheavy nuclei**

**Aleksandr Parkhomenko**

Ph.D. thesis accomplished under the scientific  
supervision of  
Prof. dr hab. Adam Sobiczewski

Warsaw 2006



# Contents

<b>1</b>	<b>Introduction</b>	<b>5</b>
<b>2</b>	<b>Method of the calculations</b>	<b>9</b>
2.1	Nuclear mass . . . . .	9
2.2	Macroscopic energy . . . . .	9
2.3	Microscopic energy . . . . .	11
2.3.1	Shell correction . . . . .	11
2.3.2	Pairing correction . . . . .	14
2.4	Woods-Saxon potential . . . . .	21
2.5	Deformation space . . . . .	22
2.6	One-quasiparticle excitations . . . . .	24
2.7	$\alpha$ -decay energy . . . . .	25
2.8	$\alpha$ -decay half-lives . . . . .	27
2.9	Parameters of the model . . . . .	29
<b>3</b>	<b>Results and discussion</b>	<b>31</b>
3.1	One-quasiparticle excitations . . . . .	31
3.1.1	Proton one-quasiparticle states . . . . .	32
3.1.2	Neutron one-quasiparticle states . . . . .	39
3.1.3	Discussion . . . . .	45
3.2	$\alpha$ -decay half-lives of heaviest nuclei . . . . .	47
3.2.1	Discussion . . . . .	48
3.3	Interpretation of odd- $A$ $\alpha$ - decay chains . . . . .	55

---

3.3.1	$^{269}\text{Ds}$ . . . . .	57
3.3.2	$^{271}\text{Ds}$ . . . . .	59
<b>4</b>	<b>Conclusions</b>	<b>61</b>
	<b>Acknowledgements</b>	<b>63</b>
<b>5</b>	<b>Appendix</b>	<b>65</b>
5.1	Least-square method . . . . .	65
5.2	Probabilities of $\alpha$ -decays and $\gamma$ -decays . . . . .	67
5.2.1	Estimating the probabilities of $\alpha$ -decay . . . . .	67
5.2.2	Estimating the probabilities of $\gamma$ -decay . . . . .	69
	<b>Bibliography</b>	<b>71</b>

# Chapter 1

## Introduction

There are about 264 stable nuclei in nature (Fig 1.1), representing isotopes of elements containing from one to at most 94 protons. Some 2400 unstable nuclei have been made artificially during the past 70 years. The artificial elements, synthesized in scientific laboratories, have at present the atomic numbers up to  $Z=118$ .

Presently, by superheavy nuclei (SHN), one usually understands nuclei which exist just due to their shell structure [1–3]. As description of shell structure and its effects on half-lives of nuclei depend on the approach used, this definition is not sharp. All realistic descriptions, however, indicate that these are roughly nuclei with atomic number  $Z \gtrsim 104$ , i.e. nuclei of transactinide elements.

Problem of SHN has been raised in the middle of 1960-ties in the paper [4]. The conclusion of the paper was that if one could expect a nucleus, not too much more heavy than known nuclei, with both proton and neutron (spherical) shells closed, the nucleus and its neighbours could have half-lives long enough to be observed. Without effects of these shells, the nuclei would immediately decay because of large Coulomb repulsion between protons (large  $Z$ ), as indicated by models not containing shell effects.

Theoretical studies indicated that reasonable candidates for magic numbers (closed shells), next to experimentally known:  $Z=82$  and  $N=126$ , could be:  $Z=114$  and  $N=184$  [5–7]. In consequence, many calculations of the properties (especially of half-lives) of nuclei around the nucleus  $^{298}114$  have been done (e.g. [8–11]).

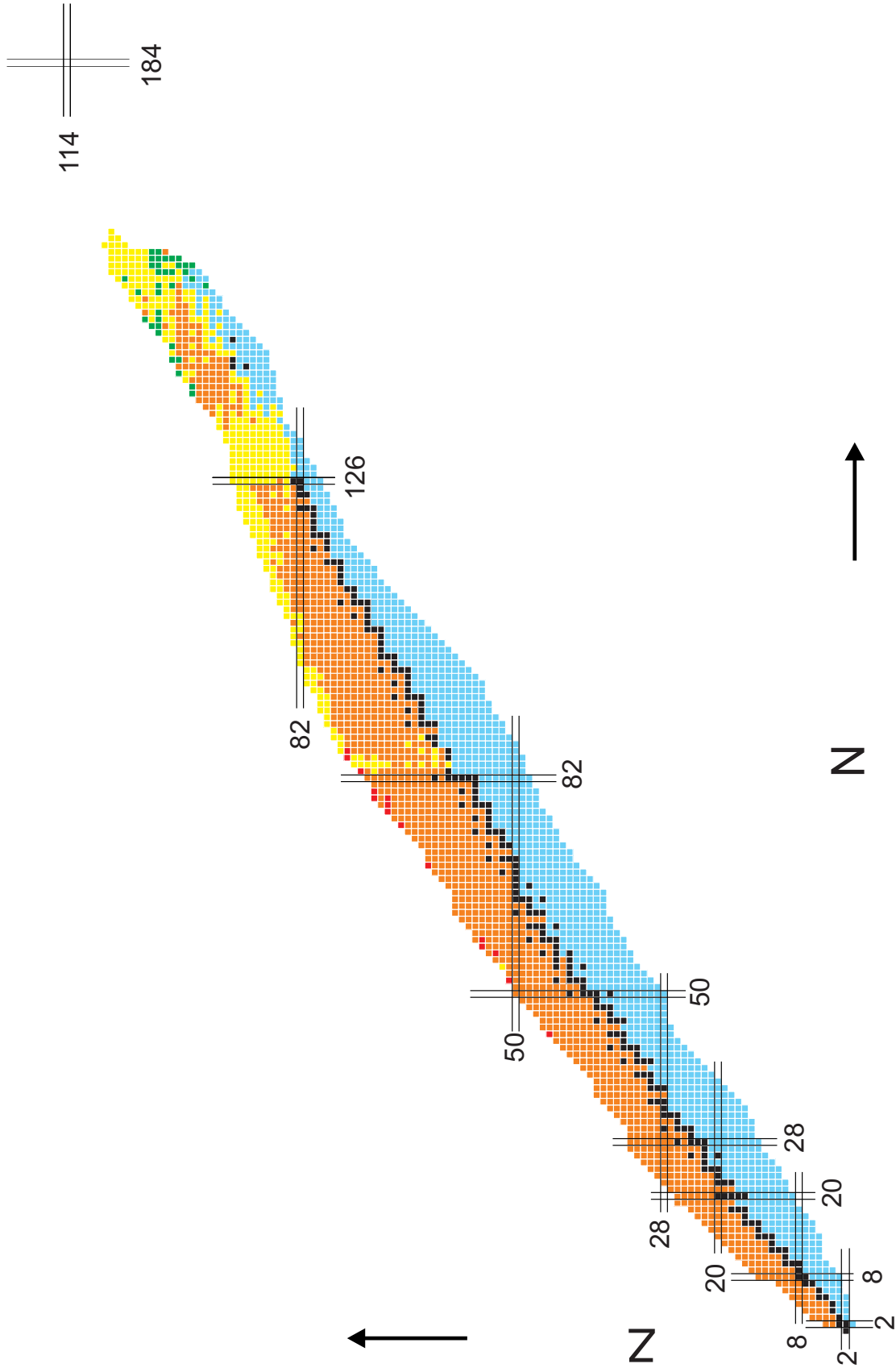


Figure 1.1: Chart of nuclides.

Later, the analysis of half-lives (e.g. [12–15]) has shown that also deformed superheavy nuclei, situated around the nucleus with  $Z=108$  and  $N=162$ , may have long enough lifetimes to be observed. Thus, properties of these nuclei are closely connected with their shell structure. In particular, significance of the shell effects is fundamental for superheavy nuclei.

Our calculations are done within a model, called macroscopic-microscopic approach, that includes shell effects and has been used by many people for a long time (e.g. [12–26]).

In the present dissertation, we concentrate on the  $\gamma$ - and  $\alpha$ -spectroscopic properties of heavy and superheavy nuclei. The  $\gamma$ -spectroscopic experimental studies, which are intensive in recent years, are done for lighter nuclei (up to rutherfordium,  $Z=104$ , e.g. [27–33]) and only approach presently the region of SHN. Thus, theoretical predictions for  $\gamma$ -spectroscopic data of these nuclei would be very helpful for an experimental identification of the excited states and their quantum characteristics. Also  $\alpha$ -spectroscopic studies are recently intensive, but mainly for the region of heaviest nuclei (e.g. [34–37]).

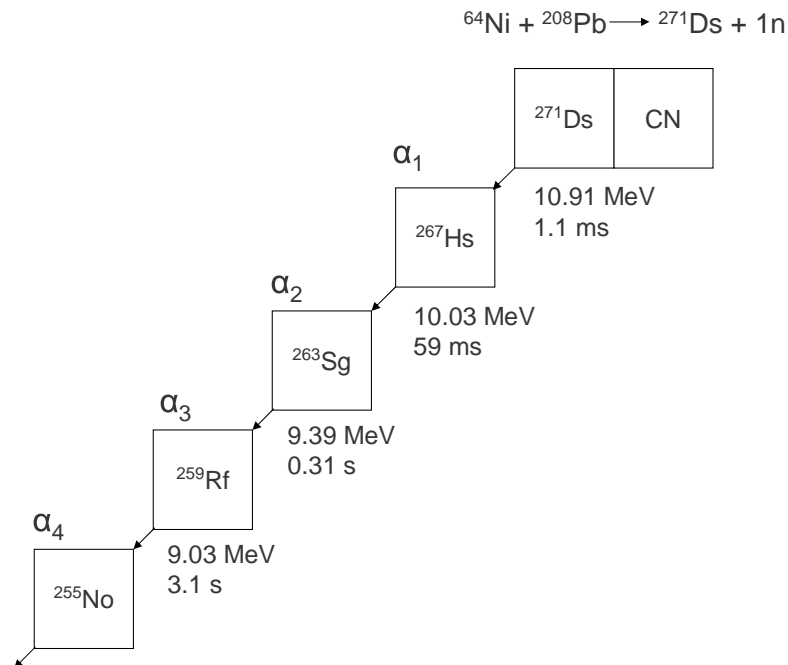


Figure 1.2: Example of the  $\alpha$ -decay chain of the nucleus  $^{271}\text{Ds}$  [38, 39].

The data come almost exclusively from measurements of  $\alpha$ -particle energies and half-lives appearing in  $\alpha$ -decay chains, mainly of odd- $A$  nuclei (see e.g. Fig 1.2). It is important then, both for the interpretation of existing data and for predictions of properties of SHN for new experiments, to realize with which accuracy one can presently describe both observables of this process:  $\alpha$ -decay energy  $Q_\alpha$  and  $\alpha$ -decay half-life  $T_\alpha$  (Fig 1.2). The energy  $Q_\alpha$  is obtained in calculations from masses of respective nuclei, which are presently described by a number of various methods (e.g. [40–44]). Half-lives  $T_\alpha$  are usually described in a phenomenological way. Microscopic description of it is a complex problem (cf. e.g. [45,46]).

There is a close connection of  $\alpha$ -spectroscopy with the  $\gamma$ -spectroscopy: using the information about excited states (their energies and quantum characteristics) of a superheavy nucleus, one can estimate the probabilities of  $\alpha$ -transition to the excited states of the daughter nucleus and compare them to the probabilities of  $\gamma$ -transitions to the states in the parent nucleus. In such a way it is possible to interpret theoretically experimental data from  $\alpha$ -decay chains. In this work probabilities of  $\alpha$ -transitions are obtained with the help of a proposed empirical five-parameter phenomenological formula, that describes  $\alpha$ -decay half-lives. Three parameters of this formula were fitted to data for even-even nuclei, and two parameters, which include averaged effect of transitions from excited states to excited states, were added for odd- $A$  groups of superheavy nuclei (one parameter for odd-even nuclei, one for even-odd). An important thing is that there are no adjustable parameters for odd-odd nuclei in the formula, since the averaged effect of transitions to excited states is taken as a sum of o-e and e-o effects. This formula and calculated neutron one-quasiparticle excitations were used in order to interpret experimental data of the  $\alpha$ -decay chains of  $^{269}\text{Ds}$  and  $^{271}\text{Ds}$ .

# Chapter 2

## Method of the calculations

### 2.1 Nuclear mass

Potential energy (mass) of nuclei has been calculated within the macroscopic-microscopic approach. Within this approach, the energy consists of two parts, macroscopic,  $E_{\text{macr}}$ , and microscopic,  $E_{\text{micr}}$

$$E_{\text{mm}} = E_{\text{macr}} + E_{\text{micr}}. \quad (2.1)$$

The macroscopic part is often calculated by means of the liquid drop model or some improvements of it [47, 48]. Both models use expansions of the energy in powers of  $A^{-1/3}$  and  $I$ , where  $I = (N - Z)/A$  is the relative neutron excess,  $Z$  is the number of protons and  $N$  is the number of neutrons in considered nucleus.

The microscopic part of the energy is a correction to the macroscopic part, which takes into account the quantum nature of a nuclear system.

### 2.2 Macroscopic energy

Smooth part of the nuclear mass is recently often used in the form of the Yukawa-plus-exponential model, formulated by Krappe and Nix [49], and has the following form:

$$\begin{aligned} M_{\text{macr}}(Z, N, \beta_\lambda^0) = & M_{\text{H}}Z + M_{\text{n}}N - a_{\text{v}}(1 - \kappa_{\text{v}}I^2)A + a_{\text{s}}(1 - \kappa_{\text{s}}I^2)A^{2/3}B_1(\beta_\lambda^0) \\ & + a_0A^0 + c_1Z^2A^{-1/3}B_3(\beta_\lambda^0) - c_4Z^{4/3}A^{-1/3} \end{aligned}$$

$$+f(k_{\text{F}}r_{\text{p}})Z^2A^{-1} - c_{\text{a}}(N - Z) - a_{\text{el}}Z^{2.39}, \quad (2.2)$$

where  $M_{\text{H}}$  is mass of the hydrogen atom,  $M_{\text{n}}$  is mass of neutron,  $A = Z + N$  is the mass number of a nucleus. The functions  $B_1(\beta_{\lambda})$  and  $B_3(\beta_{\lambda})$  describe the dependence of the surface and Coulomb energies, respectively, on the deformation  $\beta_{\lambda}$ , and  $\beta_{\lambda}^0$  is the value of the deformation at equilibrium. The formulae for  $B_1$  and  $B_3$  are [47, 48]

$$B_1 = \frac{A^{-2/3}}{8\pi^2 r_0^2 a^4} \int \int_V \left(2 - \frac{r_{12}}{a}\right) \frac{e^{-r_{12}/a}}{r_{12}/a} d^3r_1 d^3r_2, \quad (2.3)$$

$$B_3 = \frac{15}{32\pi^2} \frac{A^{-5/3}}{r_0^5} \int \int_V \frac{1}{r_{12}} \left[1 - \left(1 + \frac{1}{2} \frac{r_{12}}{a_{\text{den}}}\right) e^{-r_{12}/a_{\text{den}}}\right] d^3r_1 d^3r_2, \quad (2.4)$$

where  $r_{12} = |\vec{r}_1 - \vec{r}_2|$  with  $\vec{r}_1$  and  $\vec{r}_2$  describing the positions of two interacting volume elements,  $a$  is the range of the Yukawa interaction on which the model is based,  $a_{\text{den}}$  is the range of the Yukawa function used to generate nuclear charge distribution. The functions are normalized in such a way that they are equal to 1 for a spherical nucleus in the limit cases of  $a=0$  (for  $B_1$ ) and  $a_{\text{den}}=0$  (for  $B_3$ ), corresponding to the traditional liquid-drop model with a sharp surface. The integration is over the volume of a nucleus. The quantities  $c_1$  and  $c_4$  appearing in the Coulomb energy and the Coulomb exchange correction, respectively, are

$$c_1 = \frac{3}{5} \frac{e^2}{r_0}, \quad c_4 = \frac{5}{4} \left(\frac{3}{2\pi}\right)^{2/3} c_1, \quad (2.5)$$

where  $e$  is the elementary electric charge and  $r_0$  is the nuclear-radius parameter. The quantity  $f(k_{\text{F}}r_{\text{p}})$  appearing in the proton form-factor correction to the Coulomb energy in Eq. (2.2) has the form

$$f(k_{\text{F}}r_{\text{p}}) = -\frac{1}{8} \frac{e^2 r_{\text{p}}^2}{r_0^3} \left[ \frac{145}{48} - \frac{327}{2880} (k_{\text{F}}r_{\text{p}})^2 + \frac{1527}{1\,209\,600} (k_{\text{F}}r_{\text{p}})^4 \right], \quad (2.6)$$

where the Fermi wave number is

$$k_{\text{F}} = \left(\frac{9\pi Z}{4A}\right)^{1/3} r_0^{-1}, \quad (2.7)$$

and  $r_{\text{p}}$  is the proton root-mean-square radius. The last term in Eq. (2.2) describes the binding energy of electrons and  $a_{\text{v}}$ ,  $\kappa_{\text{v}}$ ,  $a_{\text{s}}$ ,  $\kappa_{\text{s}}$ ,  $a_0$ ,  $c_{\text{a}}$  are adjustable parameters. Thus, only two of these parameters ( $a_{\text{s}}$  and  $\kappa_{\text{s}}$ ) appear at the term, which depends on deformation. The four remaining parameters stand at the terms independent of the shape of a nucleus.

## 2.3 Microscopic energy

The microscopic part of energy consists of shell and pairing corrections to the macroscopic part:

$$E_{\text{micr}} = E_{\text{sh}}^{\text{corr}} + E_{\text{pair}}^{\text{corr}}. \quad (2.8)$$

These corrections are sums of the respective contributions from neutrons and protons, calculated separately. For a given nucleus, the microscopic energy calculated from single-particle energies gives the fluctuations of the potential energy as function of proton,  $Z$ , neutron,  $N$ , and deformation,  $\beta_\lambda$ , around its smooth trend represented by the macroscopic term.

### 2.3.1 Shell correction

The origin of the shell correction is the oscillation in the distribution of single-particle levels relative to average distribution of these levels. The correction to energy of a nucleus is the difference between two energies of it: one when it has shell structure and the other when it does not have (Fig. 2.1). We see in the figure that if the Fermi level is situated above a closed shell, the nucleus has more binding than on the average, while it has less binding than on the average when the level is below. In this way binding energy, corresponding to the case of the shell structure (a) oscillates around energy given by the uniform distribution (b).

The shell correction is calculated for a given nucleus at a given deformation within the method proposed by Strutinsky in 1966 [50, 51]. In this approach, the shell correction for a specified number  $N$  of neutrons or protons is given by the equation:

$$E_{\text{sh}}^{\text{corr}} = \sum_{\nu=1}^N \epsilon_\nu - \left\langle \sum_{\nu=1}^N \epsilon_\nu \right\rangle. \quad (2.9)$$

In the shell model, the level density can be written as:

$$\rho(\varepsilon) = \sum_{\nu} \delta(\varepsilon - \varepsilon_\nu), \quad (2.10)$$

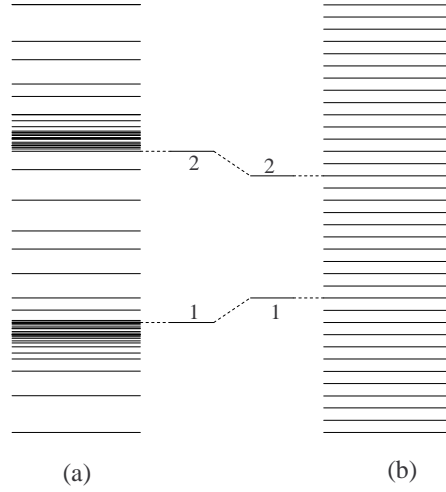


Figure 2.1: Comparison of a schematic shell structure (a) to an equally spaced level density (b). For the Fermi level (1), the binding in (a) is stronger than in (b), whereas for (2) the opposite is true.

and then the particle number is

$$N = \int_{-\infty}^{\varepsilon_F} \rho(\varepsilon) d\varepsilon, \quad (2.11)$$

where  $\varepsilon_F$  is the Fermi energy defined by this equation. As

$$\sum_{\nu=1}^N \epsilon_\nu = \int_{-\infty}^{\varepsilon_F} \rho(\varepsilon) \varepsilon d\varepsilon, \quad (2.12)$$

and, in an analogy,

$$\left\langle \sum_{\nu=1}^N \epsilon_\nu \right\rangle = \int_{-\infty}^{\tilde{\varepsilon}_F} \tilde{\rho}(\varepsilon) \varepsilon d\varepsilon \quad (2.13)$$

with the averaged part  $\tilde{\rho}(\varepsilon)$  of the exact level density  $\rho(\varepsilon)$ , the Fermi energy  $\tilde{\varepsilon}_F$ , corresponding to the smoothed, averaged density  $\tilde{\rho}(\varepsilon)$ , is defined by the equation:

$$N = \int_{-\infty}^{\tilde{\varepsilon}_F} \tilde{\rho}(\varepsilon) d\varepsilon. \quad (2.14)$$

The level density in three-dimensional potential depends on the energy in non-linear way. Such growth is not smooth, and because of levels group in shells, one can imagine

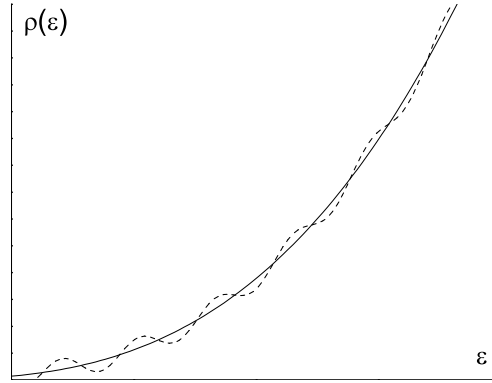


Figure 2.2: Partly (dashed line) and fully smoothed  $\rho(\varepsilon)$  (solid line).

”smooth” density (solid line) and oscillating (dashed line) part similar to those on Fig. 2.2. The averaging of  $\rho(\varepsilon)$  is done by a folding procedure:

$$\tilde{\rho}(\varepsilon) = \frac{1}{\gamma} \int_{-\infty}^{\infty} \rho(\varepsilon') f\left(\frac{\varepsilon' - \varepsilon}{\gamma}\right) d\varepsilon', \quad (2.15)$$

where  $f$  is a Gaussian-type smearing function. The width  $\gamma$  of the Gaussian function characterizes the degree of smearing. When  $\gamma$  is small,  $\rho(\varepsilon)$  is an oscillating function (dashed line in Fig. 2.2), but when it is large, of the order of the distance between shells, the smearing is full (solid line in Fig. 2.2). Full averaging procedure should leave the ”smoothed”  $\tilde{\rho}(\varepsilon)$  unchanged:

$$\tilde{\rho}(\varepsilon) = \frac{1}{\gamma} \int_{-\infty}^{\infty} \tilde{\rho}(\varepsilon') f\left(\frac{\varepsilon' - \varepsilon}{\gamma}\right) d\varepsilon'. \quad (2.16)$$

For  $f$  being  $\delta$ -function, equation (2.16) is satisfied automatically, but it is not for arbitrary function  $f$ .

We can formally expand  $\delta$ -function in the Hermite polynomials:

$$\delta(x) = \frac{1}{\sqrt{\pi}} \sum_{n=0}^{\infty} C_n H_n(x) e^{-x^2}. \quad (2.17)$$

Multiplying both sides of equation (2.17) by  $H_m(x)$ , integrating from 0 to  $\infty$  and taking into account the normalization condition

$$\int_{-\infty}^{\infty} H_m(x) H_n(x) e^{-x^2} dx = \sqrt{\pi} 2^n n! \delta_{nm}, \quad (2.18)$$

we obtain expansion coefficients  $C_m$ :

$$C_m = \frac{1}{2^m m!} H_m(0) = \begin{cases} \frac{(-1)^{\frac{m}{2}}}{2^m (\frac{m}{2})!} & \text{for even } m \\ 0 & \text{for odd } m. \end{cases} \quad (2.19)$$

Since the essential contributions to the integral (2.16) come from the region close to the point  $\varepsilon' = \varepsilon$ , we can limit the expansion (2.17) to the first  $2M$  terms:

$$\delta_{\text{cut}}(x) = \frac{1}{\sqrt{\pi}} \sum_{n=0}^{2M} C_n H_n(x) e^{-x^2}. \quad (2.20)$$

Using  $\delta_{\text{cut}}(x)$  instead of (2.17) for the function  $f$  in Eq. (2.16), the averaged density  $\tilde{\rho}$  can be obtained in the following form:

$$\tilde{\rho}(\varepsilon) = \frac{1}{\gamma \sqrt{\pi}} \sum_{\nu=1} e^{-u_\nu^2} \sum_{n=0}^{2M} C_n H_n(u_\nu), \quad (2.21)$$

with  $u_\nu = (\varepsilon - \varepsilon_\nu)/\gamma$ .

In general, the energy (2.13) will depend on the parameters  $\gamma$  and  $M$ , because the expansion (2.20) was used instead of (2.17). This approach will be meaningful only, if there is a certain interval of  $\gamma$  for fixed  $M$  within which  $\tilde{E}_{\text{sh}}$  does not depend on  $\gamma$  ("plateau condition"). For an arbitrary distribution of single-particle levels, there is no such plateau, but for physically meaningful distributions one can expect that it exists, since there is always a certain shell structure of levels with a frequency of roughly  $\hbar\omega_0$ .

### 2.3.2 Pairing correction

The second part of the microscopic correction, called pairing correction, arises due to the presence of short-range forces between correlated nucleons moving in time-reversed orbits, which cannot be included into the mean-field approach.

A proper description of a number of nuclear properties (such as the energy gap in even-even nuclei, level density, moments of inertia, etc.) is impossible without taking into account of such a short-range interaction.

### Pairing correlations in nuclei

Let us introduce operators of creation and annihilation of particle in a state  $\nu$ ,  $\hat{a}_\nu^+$  and  $\hat{a}_\nu$ . Since the nucleons are fermions, these operators satisfy the relations:

$$\{\hat{a}_\mu^+, \hat{a}_\nu^+\} = \{\hat{a}_\mu, \hat{a}_\nu\} = 0, \quad \{\hat{a}_\mu^+, \hat{a}_\nu\} = \delta_{\mu\nu}. \quad (2.22)$$

The wave function  $|0\rangle$  of the vacuum state of nucleons can be obtained from the equation:

$$\hat{a}_\nu|0\rangle = |0\rangle. \quad (2.23)$$

Then, it is possible to express single-particle wave functions  $|\nu\rangle$  by means of vacuum wave function and nucleon creation operators in the following way:

$$|\nu\rangle = \hat{a}_\nu^+|0\rangle. \quad (2.24)$$

Assuming a constant matrix element  $G$  of the short-range pairing interaction, the hamiltonian describing a system of particles may be written:

$$\hat{H} = \sum_{\nu} \varepsilon_{\nu} \hat{a}_{\nu}^+ \hat{a}_{\nu} - G \sum_{\nu, \nu' > 0} \hat{a}_{\nu}^+ \hat{a}_{\nu'}^+ \hat{a}_{\nu'} \hat{a}_{\bar{\nu}}, \quad (2.25)$$

where  $\varepsilon_{\nu}$  is the energy of a nucleon in the state  $\nu$ . The sum in Eq. (2.25) is taken over only positive values of spin projections of the states of each pair. For all states  $\nu$ , there are time-conjugated states  $\bar{\nu}$  with the same energy and opposite spin projection, which will be denoted in the future as  $-\nu$ .

The hamiltonian (2.25) describes a system of  $N$  particles, where  $N$  is the eigenvalue of the operator:

$$\hat{N} = \sum_{\nu} \hat{a}_{\nu}^+ \hat{a}_{\nu}. \quad (2.26)$$

Let us consider hamiltonian:

$$\hat{H}' = \hat{H} - \lambda \hat{N}, \quad (2.27)$$

where  $\lambda$  is the Lagrange multiplier. Bearing in mind the fact of strong correlation between nucleons in the conjugated states, it is possible to pass from the system of interacting nucleons to the system of quasiparticles, the interaction of which can be neglected.

### The Bogoliubov-Valatin transformation

Such a procedure can be done by introducing quasiparticle operators which are the linear combination of the particle operators [52–54]:

$$\begin{aligned}\hat{\alpha}_\nu^+ &= u_\nu \hat{a}_\nu^+ - v_\nu \hat{a}_{-\nu}, & \hat{\alpha}_\nu &= u_\nu \hat{a}_\nu - v_\nu \hat{a}_{-\nu}^+, \\ \hat{\alpha}_{-\nu}^+ &= u_\nu \hat{a}_{-\nu}^+ + v_\nu \hat{a}_\nu, & \hat{\alpha}_{-\nu} &= u_\nu \hat{a}_{-\nu} + v_\nu \hat{a}_\nu^+, \end{aligned}\quad (2.28)$$

where  $u_\nu$  and  $v_\nu$  are real numbers, connected with each other by the condition:

$$u_\nu^2 + v_\nu^2 = 1. \quad (2.29)$$

This transformation is called the Bogoliubov-Valatin transformation. The quasiparticle operators  $\hat{\alpha}_\nu^+$  and  $\hat{\alpha}_\nu$  satisfy the same commutation relations (2.22) as those for operators of particle creation and annihilation:

$$\{\hat{\alpha}_\mu^+, \hat{\alpha}_\nu^+\} = \{\hat{\alpha}_\mu, \hat{\alpha}_\nu\} = 0, \quad \{\hat{\alpha}_\mu^+, \hat{\alpha}_\nu\} = \delta_{\mu\nu}. \quad (2.30)$$

The inverse transformation is given by:

$$\begin{aligned}\hat{a}_\nu^+ &= u_\nu \hat{\alpha}_\nu^+ + v_\nu \hat{\alpha}_{-\nu}, & \hat{a}_\nu &= u_\nu \hat{\alpha}_\nu - v_\nu \hat{\alpha}_{-\nu}^+, \\ \hat{a}_{-\nu}^+ &= u_\nu \hat{\alpha}_{-\nu}^+ - v_\nu \hat{\alpha}_\nu, & \hat{a}_{-\nu} &= u_\nu \hat{\alpha}_{-\nu} + v_\nu \hat{\alpha}_\nu^+. \end{aligned}\quad (2.31)$$

Putting (2.31) into (2.27), the hamiltonian takes the form:

$$\hat{H}' = E_0 + \sum_\nu E_\nu \hat{\alpha}_\nu^+ \hat{\alpha}_\nu + \hat{H}_{20} + \hat{H}_{int}, \quad (2.32)$$

where

$$E_\nu = \sqrt{(\varepsilon_\nu - \lambda)^2 + \Delta^2}, \quad (2.33)$$

$E_0$  is a constant, which is independent of operators of quasiparticles:

$$E_0 = \sum_\nu (\varepsilon_\nu \cdot 2v_\nu^2 - Gv_\nu^4) - \Delta^2/G, \quad (2.34)$$

and

$$\Delta = G \sum_{\nu>0} u_\nu v_\nu. \quad (2.35)$$

The term  $\hat{H}_{20}$  is given by:

$$\hat{H}_{20} = \sum_{\nu>0} [2u_{\nu}v_{\nu}(\varepsilon_{\nu} - \lambda) - \Delta(u_{\nu}^2 - v_{\nu}^2)] (\hat{\alpha}_{\nu}^{+}\hat{\alpha}_{-\nu}^{+} + \hat{\alpha}_{-\nu}\hat{\alpha}_{\nu}). \quad (2.36)$$

The last term in Eq. (2.32),  $\hat{H}_{int}$ , contains products of 4 quasiparticle operators. Neglecting the interaction between quasiparticles  $\hat{H}_{int}$  and putting  $\hat{H}_{20} = 0$ , the hamiltonian of the system becomes the hamiltonian of free quasiparticles. The requirement that the  $\hat{H}_{20}$  term disappears,

$$2u_{\nu}v_{\nu}(\varepsilon_{\nu} - \lambda) - \Delta(u_{\nu}^2 - v_{\nu}^2) = 0, \quad (2.37)$$

with the condition (2.29) leads to two solutions for  $v_{\nu}^2$  and  $u_{\nu}^2$ :

$$\begin{cases} u_{\nu}^2 = \frac{1}{2} \left( 1 + \frac{\varepsilon_{\nu} - \lambda}{E_{\nu}} \right), \\ v_{\nu}^2 = \frac{1}{2} \left( 1 - \frac{\varepsilon_{\nu} - \lambda}{E_{\nu}} \right). \end{cases} \quad (2.38)$$

The particle number operator (2.26) can be written in terms of quasiparticles:

$$\hat{N} = 2 \sum_{\nu>0} v_{\nu}^2 + \sum_{\nu>0} (u_{\nu}^2 - v_{\nu}^2) (\hat{\alpha}_{\nu}^{+}\hat{\alpha}_{\nu} + \hat{\alpha}_{-\nu}^{+}\hat{\alpha}_{-\nu}) + \sum_{\nu>0} 2u_{\nu}v_{\nu} (\hat{\alpha}_{\nu}^{+}\hat{\alpha}_{-\nu}^{+} + \hat{\alpha}_{-\nu}\hat{\alpha}_{\nu}), \quad (2.39)$$

and the number of particles in the ground state of the system (i.e. in the state without quasiparticles) is

$$N = 2 \sum_{\nu>0} v_{\nu}^2. \quad (2.40)$$

Using (2.38), this can be written as

$$N = \sum_{\nu>0} \left[ 1 - \frac{\varepsilon_{\nu} - \lambda}{\sqrt{(\varepsilon_{\nu} - \lambda)^2 + \Delta^2}} \right]. \quad (2.41)$$

Inserting (2.38) into (2.35), we obtain the second of the system of two BCS equations for the parameters  $\lambda$  and  $\Delta$  (for  $\Delta \neq 0$ ):

$$\frac{2}{G} = \sum_{\nu>0} \frac{1}{\sqrt{(\varepsilon_{\nu} - \lambda)^2 + \Delta^2}}, \quad (2.42)$$

where  $\lambda$  is a chemical potential, Eq. (2.27), and  $\Delta$  is the energy gap parameter (as will become clear later).

If non-trivial solution ( $\Delta \neq 0$ ) of BCS equations (2.42) and (2.41) exists, the condition

$$\sqrt{(\varepsilon_\nu - \lambda)^2 + \Delta^2} > |\varepsilon_\nu - \lambda|, \quad (2.43)$$

has to be fulfilled. Inserting (2.43) into (2.42), we obtain

$$\frac{2}{G} = \sum_{\nu>0} \frac{1}{\sqrt{(\varepsilon_\nu - \lambda)^2 + \Delta^2}} < \sum_{\nu>0} \frac{1}{|\varepsilon_\nu - \lambda|}, \quad (2.44)$$

and, thus,

$$G > 2 \left( \sum_{\nu>0} \frac{1}{|\varepsilon_\nu - \lambda|} \right)^{-1} \equiv G_{\text{cr}}. \quad (2.45)$$

In the BCS approximation, there are no physical solutions for pairing strengths  $G < G_{\text{cr}}$ . Figure 2.3 shows the dependence of the pairing gap parameter  $\Delta_p$ , calculated for the system with 108 protons ( $^{263}\text{Hs}$ ), on the pairing strength  $G_p$ . Dashed line is a "real" behavior and the solid one shows the dependence of  $\Delta_p$  on  $G_p$  in the BCS approximation. One can see that the BCS approximation does not have non-trivial solutions for  $G < G_{\text{cr}}$ . Such a break of the BCS solutions for  $\Delta$  ( $\Delta_p = 0$  or close to 0) takes place for nuclei in the vicinity of closed shells.

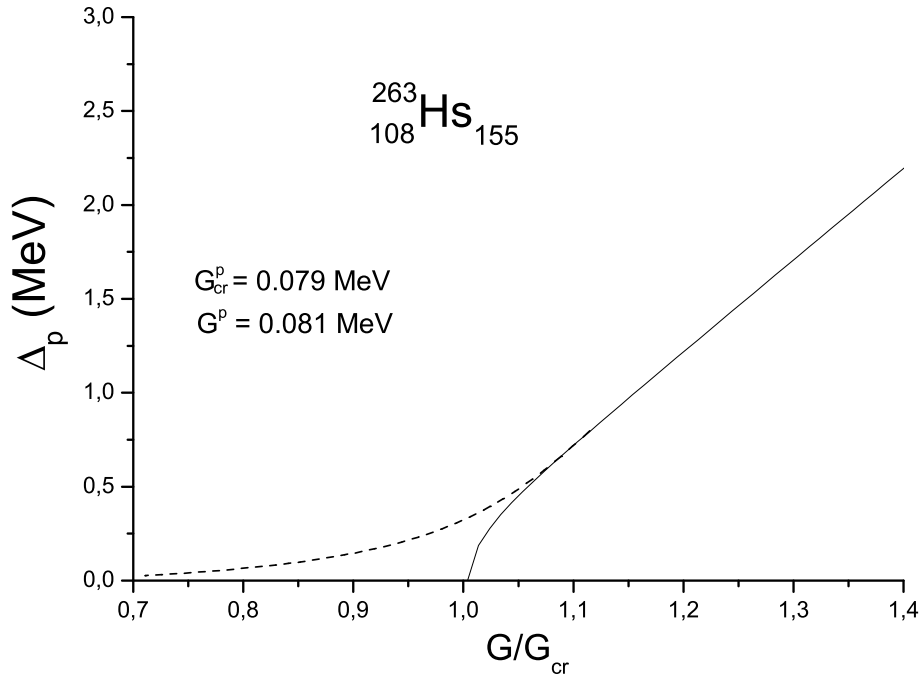


Figure 2.3: Dependence of the pairing gap parameter  $\Delta_p$  on the pairing strength  $G_p$  for  $^{263}\text{Hs}$ .

### Wave functions and the energy spectrum

The BCS wave function has the following form:

$$|BCS\rangle = \prod_{\nu>0} (u_\nu + v_\nu \hat{a}_\nu^+ \hat{a}_{-\nu}^+) |0\rangle. \quad (2.46)$$

It is the wave function of vacuum for quasiparticles. From Eq. (2.46), one can also conclude that  $2v_\nu^2$  is the probability that the coupled states  $|\nu\rangle$  and  $|-\nu\rangle$  are occupied by a pair of nucleons;  $2u_\nu^2$  is the probability that these states are not occupied. For the energy of the system in its ground state, one gets in the BCS approach:

$$E_{\text{BCS}} = \langle BCS | \hat{H} | BCS \rangle = 2 \sum_{\nu>0} \varepsilon_\nu v_\nu^2 - \frac{\Delta^2}{G} - G \sum_{\nu>0} v_\nu^4. \quad (2.47)$$

It is the state of the vacuum of quasiparticles with the energy  $E_0 = E_{\text{BCS}}$ , Eq. (2.34). The hamiltonian of free quasiparticles, as was shown earlier, can be written:

$$H = E_{\text{BCS}} + \sum_{\nu} E_\nu \hat{\alpha}_\nu^+ \hat{\alpha}_\nu \quad (2.48)$$

with the quasiparticle energy  $E_\nu$  given by Eq. (2.33). This energy may be written as the difference:

$$E_\nu = \langle BCS | \hat{\alpha}_\nu \hat{H} \hat{\alpha}_\nu^+ | BCS \rangle - \langle BCS | \hat{H} | BCS \rangle, \quad (2.49)$$

and corresponds to the one-quasiparticle state  $\hat{\alpha}_\nu^+ | BCS \rangle$ . It is a state with odd particle number and therefore describes a nucleus with an odd number of nucleons. The lowest value of  $E_\nu$  corresponds to the ground state of an odd nucleus, all other values of  $E_\nu$  correspond to its excited states. Similarly, one can speak about two-quasiparticle states, which describe excitations of even system:

$$E_{\nu_1 \nu_2} = \langle BCS | \hat{\alpha}_{\nu_1} \hat{\alpha}_{\nu_2} \hat{H} \hat{\alpha}_{\nu_1}^+ \hat{\alpha}_{\nu_2}^+ | BCS \rangle - \langle BCS | \hat{H} | BCS \rangle = E_{\nu_1} + E_{\nu_2}, \quad (2.50)$$

or

$$E_{\nu_1 \nu_2} = \sqrt{(\varepsilon_{\nu_1} - \lambda)^2 + \Delta^2} + \sqrt{(\varepsilon_{\nu_2} - \lambda)^2 + \Delta^2}. \quad (2.51)$$

Thus, in the even system the first excited state lies by at least  $2\Delta$  higher than the ground state and that is why  $\Delta$  is called the energy gap parameter.

### Pairing correction

Pairing correction energy  $E_{\text{pair}}^{\text{corr}}$  of Eq. (2.8) is constructed in a full analogy to the shell correction energy  $E_{\text{sh}}^{\text{corr}}$ . It is

$$E_{\text{pair}}^{\text{corr}} = E_{\text{pair}} - \tilde{E}_{\text{pair}}, \quad (2.52)$$

where  $E_{\text{pair}}$  is the pairing energy corresponding to real single-particle level distribution  $\rho(\varepsilon)$ , Eq. (2.10), and  $\tilde{E}_{\text{pair}}$  is this energy, when the distribution is smoothed,  $\tilde{\rho}(\varepsilon)$ , Eq. (2.15).

The energy  $E_{\text{pair}}$  is

$$E_{\text{pair}} = E_{\text{BCS}} - E_{\text{BCS}}^{\Delta=0}, \quad (2.53)$$

where  $E_{\text{BCS}}^{\Delta=0}$  is the  $E_{\text{BCS}}$  energy in the limit of disappearing pairing correlations ( $\Delta = 0$ ). Thus, using Eq. (2.47),

$$E_{\text{BCS}}^{\Delta=0} = 2 \sum_{\nu=1}^{N/2} \varepsilon_{\nu} - \frac{GN}{2}, \quad (2.54)$$

because in the case of  $\Delta = 0$ , the probability  $v_{\nu}^2$  of the occupation of a state  $\nu$  is

$$v_{\nu}^2 = \begin{cases} 0 & \text{for } \nu \text{ above the Fermi level} \\ 1 & \text{for } \nu \text{ below the Fermi level,} \end{cases} \quad (2.55)$$

according to Eq. (2.38).

A relatively simple expression for the energy  $\tilde{E}_{\text{pair}}$  can be obtained, when only the first term in the Taylor expansion of the smoothed single-particle energy, treated as a function of particle number  $n$  around the Fermi level  $\tilde{\varepsilon}_{\text{F}}$ , is taken

$$\tilde{\varepsilon}(n) = \tilde{\varepsilon}_{\text{F}} + \frac{1}{\tilde{\rho}_{\text{F}}}(n - N), \quad (2.56)$$

where  $\tilde{\rho}_{\text{F}}$  is the smoothed level density at the Fermi level  $\tilde{\rho}(\tilde{\varepsilon}_{\text{F}})$ . The expression is [55]

$$\tilde{E}_{\text{pair}} = -\frac{1}{2} \frac{N^2}{\tilde{\rho}_{\text{F}}} \left\{ \left[ 1 + \left( \frac{\tilde{\rho}_{\text{F}} \tilde{\Delta}}{N} \right)^2 \right]^{1/2} - 1 \right\} + \frac{1}{4} \tilde{\rho}_{\text{F}} \tilde{\Delta} G \arctan \frac{N}{\tilde{\rho}_{\text{F}} \tilde{\Delta}}, \quad (2.57)$$

where pairing strength  $G$  is related with the smoothed energy-gap parameter  $\tilde{\Delta}$  by the pairing equation [55]

$$\frac{1}{G} = \frac{1}{2} \tilde{\rho}_{\text{F}} \ln \left\{ \left[ \left( \frac{N}{\tilde{\rho}_{\text{F}} \tilde{\Delta}} \right)^2 + 1 \right]^{1/2} + \frac{N}{\tilde{\rho}_{\text{F}} \tilde{\Delta}} \right\}, \quad (2.58)$$

For the single-particle energies  $\varepsilon_\nu$ , the energies calculated in the Woods-Saxon potential have been used.

## 2.4 Woods-Saxon potential

The Woods-Saxon potential  $V_{\text{WS}}$  has the following form:

$$V_{\text{WS}}(\vec{r}) = -\frac{V}{1 + e^{d(\vec{r}, \text{def})/a_{\text{ws}}}}, \quad (2.59)$$

where  $V$  is the depth of the potential,  $d(\vec{r}, \text{def})$  is the distance from the point  $\vec{r}$  to the surface of the nucleus,  $a_{\text{ws}}$  is the diffuseness of the nuclear surface. The symbol "def" stands for deformation; it is stressed here that the distance from the nuclear surface depends on the deformation of a nucleus, that is on the deformation of the nuclear surface. The depth of the potential is

$$V = V_0(1 \pm \kappa I), \quad (2.60)$$

where  $I = (N - Z)/A$  is the relative neutron excess and  $V_0$  and  $\kappa$  are adjustable parameters. The sign (+) is for protons and (−) for neutrons.

In the case of spherical shape, the potential is

$$V_{\text{WS}}(\vec{r}) = -\frac{V}{1 + e^{(r-R_0)/a_{\text{ws}}}}, \quad (2.61)$$

where  $R_0 = r_0 A^{1/3}$ .

The full microscopic potential has the form (e.g. [56]):

$$V_{\text{micr}} = V_{\text{WS}} + \lambda \left( \frac{\hbar}{2mc} \right)^2 (\nabla V_{\text{WS}}) \cdot (\vec{\sigma} \times \vec{p}/\hbar) + V_c, \quad (2.62)$$

where the second term is the spin-orbit potential and the third term is the Coulomb potential, which has the form:

$$V_c(\vec{r}) = \rho_c \int \frac{d^3 r'}{|\vec{r} - \vec{r}'|}, \quad (2.63)$$

with  $\rho_c = (3Ze)/(4\pi R_0^3)$  and  $e$  is the elementary charge.

## 2.5 Deformation space

Shape of a nucleus, in the intrinsic frame of reference is defined by a standard deformation parameters  $\beta_{\lambda\mu}$

$$R(\theta, \phi) = R_0(\beta_{\lambda\mu}) \left( 1 + \sum_{\lambda=0}^{\infty} \sum_{\mu=-\lambda}^{\lambda} \beta_{\lambda\mu} Y_{\lambda\mu}(\theta, \phi) \right), \quad (2.64)$$

where  $Y_{\lambda\mu}(\theta, \phi)$  are spherical harmonics,  $R_0$  is radius of a spherical nucleus with the same volume as the nucleus considered (the reflection of the incompressibility of the nuclear matter).

The analysis of the equilibrium deformations has shown [57] that it is sufficient to consider the multipolarities up to  $\lambda=8$ . The contribution of  $\lambda=9$  and 10 is already negligible. The odd multipolarities  $\lambda=3,5,7$  contribute only to the deformations of light isotopes of the elements around radium [57]. Additionally, it is found that the ground-state shape of the nuclei, which we usually consider, is axially symmetric. Thus, the 4-dimensional deformation space  $\{\beta_\lambda\}$ ,  $\lambda=2,4,6,8$ , has been found to be sufficient for almost all nuclei in the considered region, in which we are usually interested, in particular for all superheavy nuclei [58] and the formula (2.64) can be rewritten:

$$R(\theta) = R_0 \left( 1 + \sum_{\lambda=2}^8 \beta_\lambda Y_\lambda(\theta) \right) \quad (2.65)$$

with  $\beta_\lambda \equiv \beta_{\lambda 0}$  and  $Y_\lambda(\theta) \equiv Y_{\lambda 0}(\theta, 0)$ .

This description of the nuclear shape is used both for the macroscopic (surface and Coulomb energies) and the microscopic (shape of single-particle potential) parts of energy.

The shapes of the nuclei are illustrated in Fig. 2.4 [59]. One can see that they vary quite much with  $Z$  and  $N$ . Some of the nuclei are thicker in their equatorial plane, some are thinner (necking), some ( $Z>120$ ) show a tendency to be oblate. Values of the equilibrium deformations  $\beta_\lambda^0$  may be found in [60, 61].

Contour maps of the equilibrium deformations  $\beta_\lambda^0$ ,  $\lambda=2,4,6,8$ , are given in Fig. 2.5, which is taken (after a small modification) from [58]. They are obtained by minimization of the energy of a nucleus in the  $\beta_\lambda$  degrees of freedom. Most of considered nuclei are deformed. Only two rather small regions of spherical nuclei appear: one (smaller) around

the doubly magic spherical nucleus  $^{208}\text{Pb}$  and the other (larger) around the predicted [5,6] strong neutron closed shell at  $N=184$ .

The main, quadrupole, component of the deformation,  $\beta_2^0$ , is largest and it is positive in almost the whole region of deformed nuclei. It is large ( $\beta_2^0 \approx 0.24$ ) and about constant in a large part of the region (around its center) and it rapidly decreases as one moves towards the boundaries of this region. The higher-multipolarity components are smaller and they change sign as one moves through the region. This situation stresses the important role of these high-multipolarity deformations, as mainly they are responsible for changes of the properties of heavy and superheavy nuclei with changes of  $Z$  and  $N$  in the large region, where the quadrupole deformation is about constant.

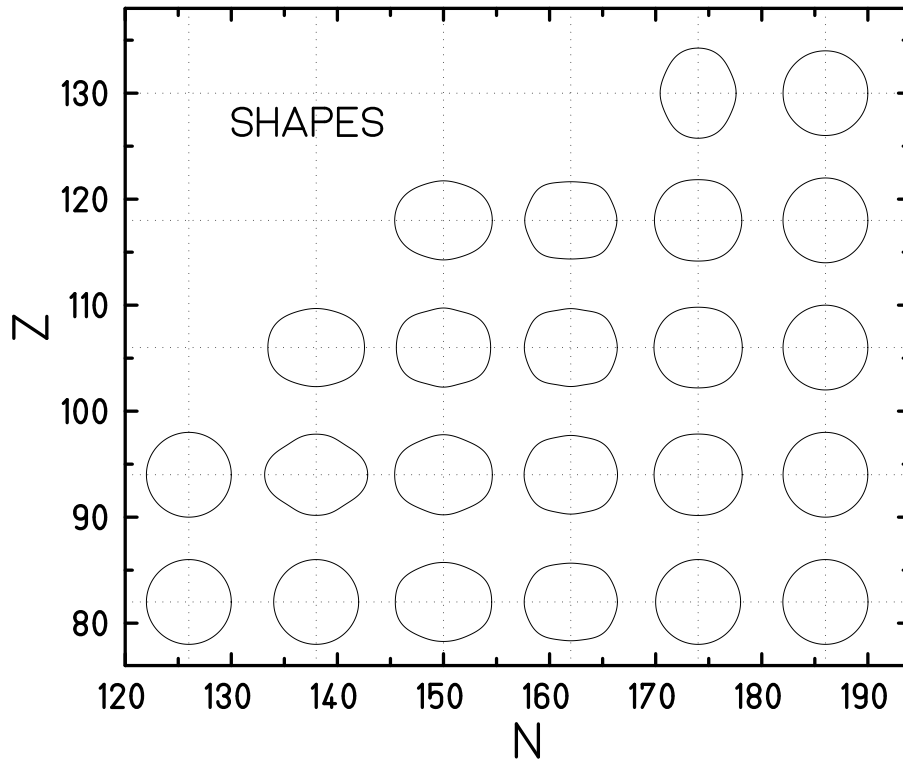


Figure 2.4: Shapes of nuclei plotted for the region of  $Z=82-130$  and  $N=126-190$  [59].

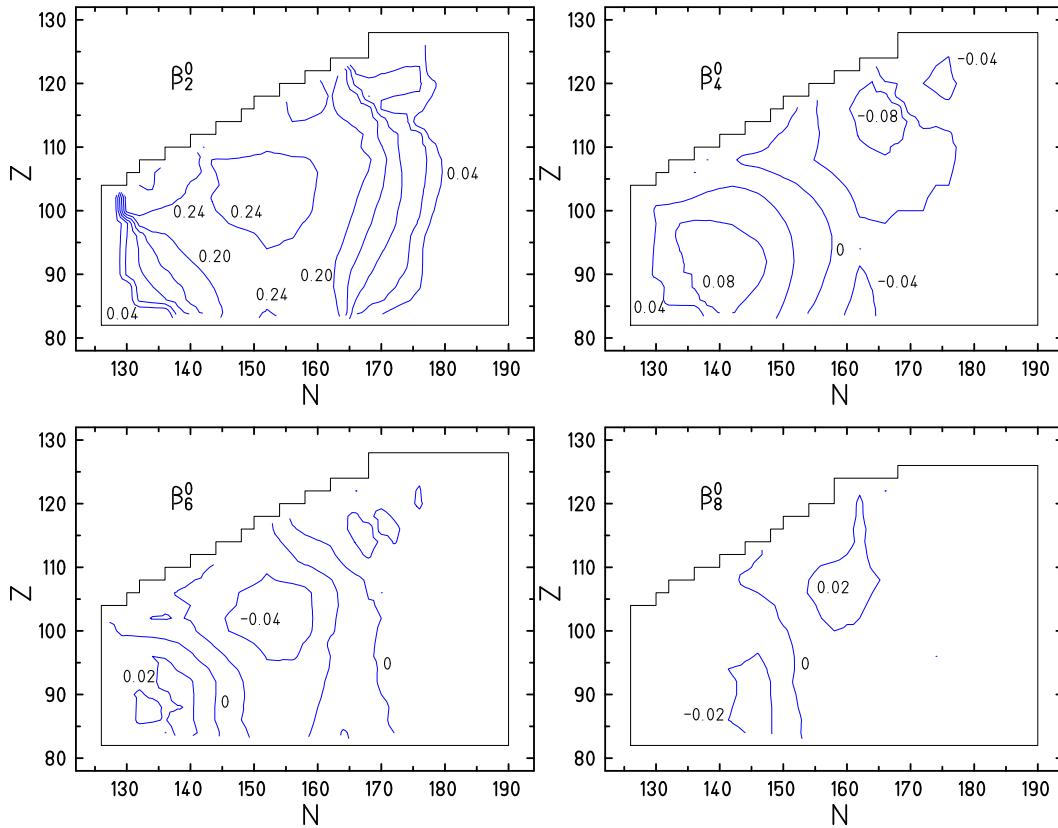


Figure 2.5: Contour maps of the equilibrium deformations  $\beta_\lambda^0$ ,  $\lambda=2,4,6,8$ , plotted as functions of proton  $Z$  and neutron  $N$  numbers. Numbers at the contour lines give the values of the deformations [58].

## 2.6 One-quasiparticle excitations

The excitation energy of one odd nucleon (Fig. 2.6) in a nucleus is given by Eq. (2.33). The lowest calculated in this way energy corresponds to the ground state of an odd- $A$  nucleus and all other correspond to excited states. The single-particle spectra for protons and neutrons have been calculated in [79, 85] using the Woods-Saxon potential. For each energy level, the quantum characteristics (projection of the total spin on the symmetry axis,  $\Omega$ , and parity  $\pi$  of the state) have been given. Besides  $\Omega$ , and  $\pi$ , also the Nilsson ("asymptotic") quantum numbers  $[Nn_z\Lambda]$  have been specified, where  $N$  is the total number

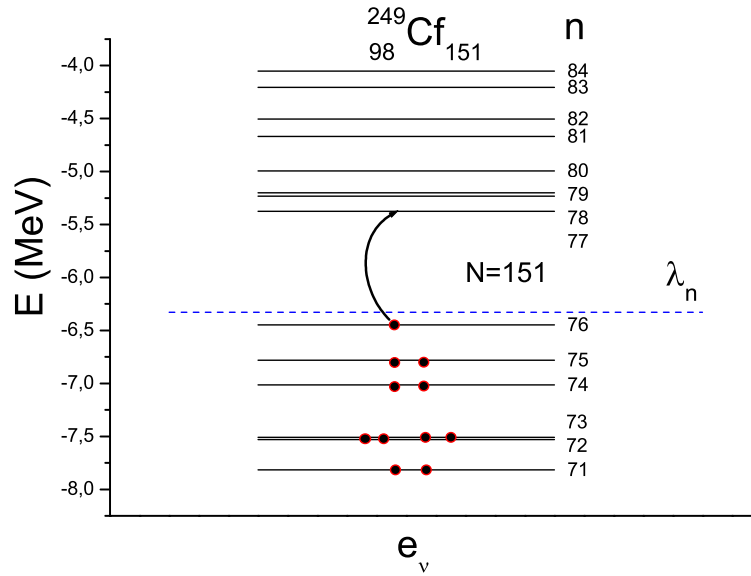


Figure 2.6: Excitation of one odd neutron in the nucleus  ${}_{98}^{249}\text{Cf}_{151}$ . Single-particle energies are calculated within the Woods-Saxon potential.

of the oscillator quanta,  $n_z$  is the number of quanta along the symmetry axis  $Oz$  and  $\Lambda$  is the projection of the orbital angular momentum on the symmetry axis.

## 2.7 $\alpha$ -decay energy

Alpha decay is one of two main decay modes of heaviest nuclei. It is especially important for these nuclei because many of already known heavy nuclei decay by this mode, and also many of nuclei not yet observed (especially superheavy nuclei) are predicted to be  $\alpha$ -emitters. Additionally, this decay supplies us with a good method for the identification of the decaying nuclei (genetic chains). Amount of already collected data for  $\alpha$  decay is quite large (e.g. [34–38, 62–66]) and is still increasing.

The  $\alpha$ -decay energy  $Q_\alpha(Z, N)$  of a nucleus with  $Z$  protons and  $N$  neutrons is

$$Q_\alpha(Z, N) = M(Z, N) - M(Z - 2, N - 2) - M_\alpha, \quad (2.66)$$

where  $M(Z, N)$  is mass of a nucleus with  $Z$  protons and  $N$  neutrons and  $M_\alpha$  is mass of

$\alpha$ -particle. This formula corresponds to the case of transitions from the ground state of the parent nucleus to the ground state of the daughter nucleus in the  $\alpha$ -decay process.

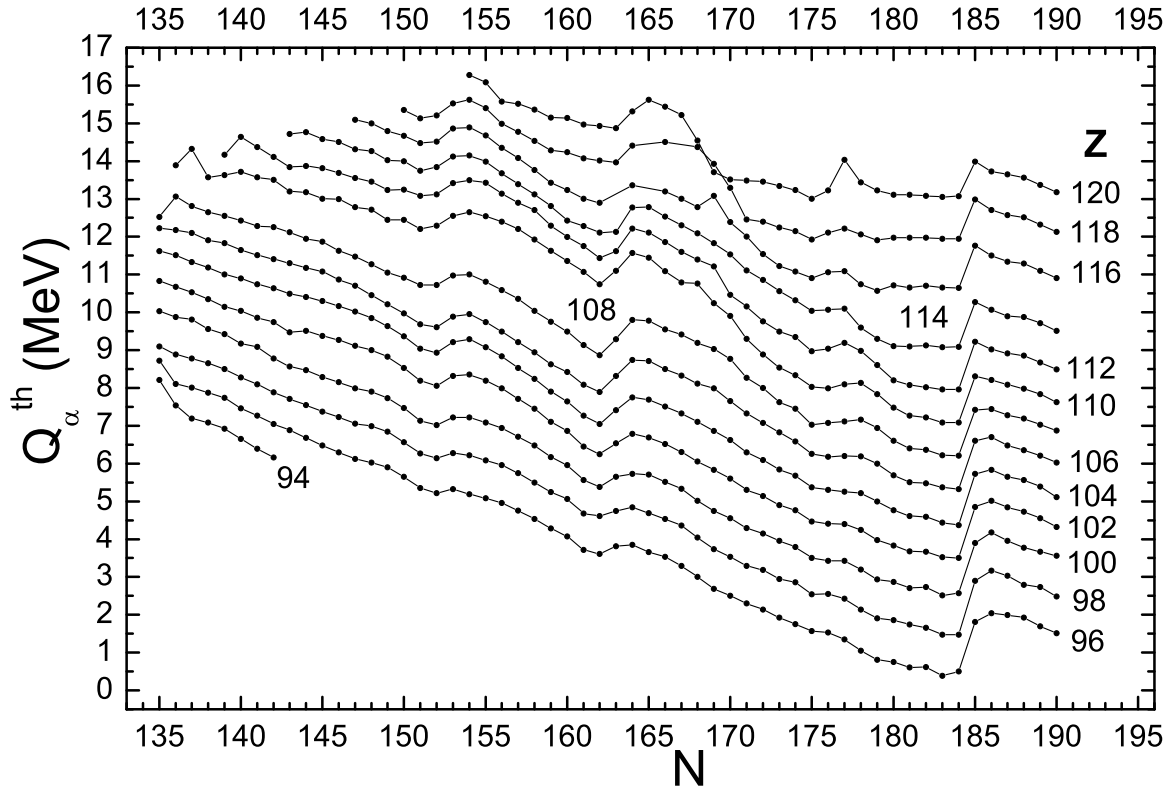


Figure 2.7: Calculated  $\alpha$ -decay energy  $Q_\alpha^{\text{th}}$  in MeV as a function of the neutron number  $N$  for elements 94-120.

To illustrate shell effects, the calculated  $\alpha$ -decay energy  $Q_\alpha$  (Eq. 2.66) for even-even nuclei is plotted as a function of the neutron number  $N$  (Fig. 2.7). The effect of the deformed neutron shell at  $N=162$  and the weaker one at  $N=152$  are clearly seen. The effect of the deformed proton shell at  $Z=108$  is also visible. The effects of the spherical shells at  $Z=114$  and  $N=184$  are also manifested.

Taking into account single-particle structure of an odd- $A$  and odd-odd nuclei, one can introduce the transition energy,  $Q_\alpha^{\text{t}}$ , remembering that the  $\alpha$ -decay can occur from excited to excited state:

$$Q_\alpha^{\text{t}} = Q_\alpha + (E_{\text{p}} - E_{\text{d}}) \equiv Q_\alpha + \Delta E, \quad (2.67)$$

where  $E_p$  and  $E_d$  are the excitation energies of initial (parent nucleus) and final (daughter nucleus) states, respectively. The quantity  $\Delta E$  is just the single-particle effect in this transition energy.

Comparing the probability of the  $\alpha$ -decay of a nucleus from the excited one-quasiparticle state with the probability of the  $\gamma$ -emission from this state, it is possible to propose the interpretation of the  $\alpha$ -decay chains (see Appendix).

## 2.8 $\alpha$ -decay half-lives

A 3-parameter formula is used in this work for even-even (e-e) nuclei. It has been obtained by reduction of one parameter in the rather old formula of Viola and Seaborg [67], which has been often used up to the present day (see e.g. [13, 14, 20, 58, 68–70]). Our formula reads:

$$\log_{10} T_\alpha = \frac{aZ}{\sqrt{Q_\alpha}} + bZ + c, \quad (2.68)$$

where  $a$ ,  $b$  and  $c$  are adjustable parameters.

In the case of odd- $A$  and o-o nuclei, structure of the ground states (g.s.) of a parent and the daughter nuclei are, in general, different. This causes a hindrance of the transition between these states. A parent nucleus prefers to decay from its g.s. to such an excited state of its daughter which has the same (or similar) structure. When we do not know the excitation energy of such a state, it is natural to treat it as an adjustable parameter. Thus, the formula (2.68), generalized to describe also odd- $A$  and o-o nuclei, takes the form

$$\log_{10} T_\alpha^{\text{ph}}(Z, N) = aZ(Q_\alpha - \bar{E}_i)^{-1/2} + bZ + c, \quad (2.69)$$

where  $\bar{E}_i=0$  for e-e nuclei,  $\bar{E}_i = \bar{E}_p$  (average excitation energy of proton one-quasiparticle state to which  $\alpha$  decay goes) for o-e nuclei,  $\bar{E}_i = \bar{E}_n$  (average excitation energy of neutron one-quasiparticle state to which  $\alpha$  decay goes) for e-o nuclei and  $\bar{E}_i = \bar{E}_{\text{pn}}$  (average excitation energy of one-proton and one-neutron quasiparticle state) for o-o nuclei. To minimize the number of adjustable parameters, we put the average excitation energy  $\bar{E}_{\text{pn}}$  of o-o nuclei as equal to the sum of the average energies of o-e ( $\bar{E}_p$ ) and e-o ( $\bar{E}_n$ ) nuclei, i.e.

$$\bar{E}_{\text{pn}} = \bar{E}_p + \bar{E}_n. \quad (2.70)$$

This way, we get only 5 adjustable parameters to describe all four classes of nuclei by the formula (2.69).

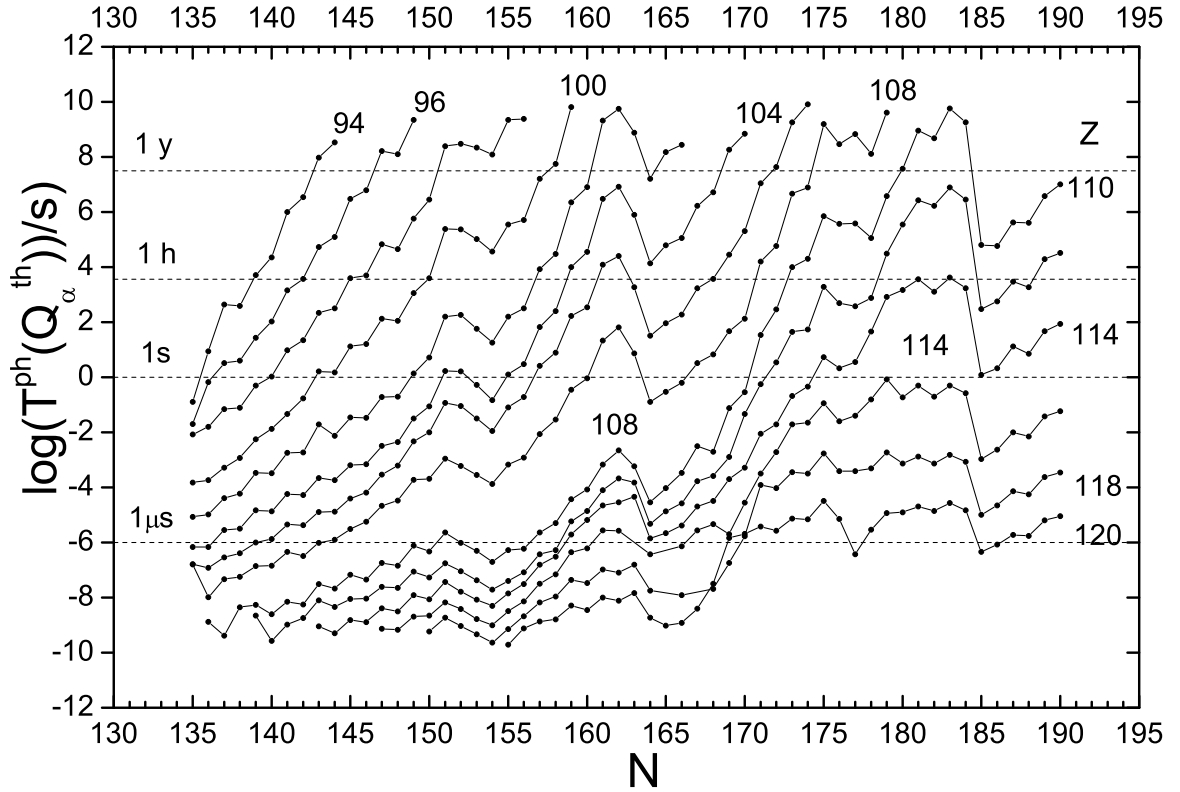


Figure 2.8: Same as in Fig. 2.7 but for logarithm of the  $\alpha$ -decay half-life  $T_\alpha(Q_\alpha^{\text{th}})$  given in seconds.

The first three ones:  $a$ ,  $b$ ,  $c$  are obtained from a fit to e-e nuclei data, the next one:  $\delta\bar{E}_p$ , from a fit to o-e data (with  $a$ ,  $b$ ,  $c$  kept the same as for e-e nuclei) and the final one:  $\delta\bar{E}_n$  from a fit to e-o data [71].

Figure 2.8 shows logarithm of the  $\alpha$ -decay half-life  $T_\alpha^{\text{ph}}(Q_\alpha^{\text{th}})$  as a function of the neutron number  $N$  for the same nuclei for which the  $\alpha$ -decay energy  $Q_\alpha^{\text{th}}$  is given in Fig. 2.7. The logarithm of the  $\alpha$ -decay half-life is calculated by means of the formula (2.69) with the parameters of Eq. (2.78). According to Eq. 2.69 the dependence of  $\log_{10}T_\alpha^{\text{ph}}(Q_\alpha^{\text{th}})$  on the proton number  $Z$  and the neutron number  $N$  is a consequence of the dependence of the  $\alpha$ -decay energy  $Q_\alpha^{\text{th}}$  on these quantities. Therefore, all shell effects seen in  $Q_\alpha^{\text{th}}$  in Fig. 2.7

are clearly reflected in  $\log_{10} T_{\alpha}^{\text{ph}}(Q_{\alpha}^{\text{th}})$  in Fig. 2.8.

## 2.9 Parameters of the model

The macroscopic part of mass, Eq. (2.2), is used the same as in [41], where 3 of its adjustable parameters:  $a_v$ ,  $\kappa_v$  and  $a_0$  were fitted to experimental masses of even-even heaviest nuclei with  $Z \geq 84$ . The result was

$$a_v = 16.0643, \quad \kappa_v = 1.9261, \quad a_0 = 17.926. \quad (2.71)$$

It was found that omission of the two terms considered in [47]: charge-asymmetry term  $c_a(N - Z)$  and Wigner term (characterized by a coefficient  $W$ ), i.e. putting

$$c_a = 0, \quad W = 0, \quad (2.72)$$

does not significantly change the quality of description of mass of heaviest nuclei. The values adopted after [47] are:

$$a_s = 21.13 \text{ MeV}, \quad \kappa_s = 2.30, \quad (2.73)$$

$$\begin{aligned} a &= 0.68 \text{ fm}, & a_{\text{den}} &= 0.70 \text{ fm}, & r_0 &= 1.16 \text{ fm}, \\ r_p &= 0.80 \text{ fm}, & a_{\text{el}} &= 1.433 \cdot 10^{-5} \text{ MeV}. \end{aligned} \quad (2.74)$$

The values of the Woods-Saxon potential, taken for the calculations of the microscopic part of mass, are (cf. [56] and also [14], where these values are also specified):

$$\begin{aligned} r_0 &= 1.275 \text{ fm}, & (r_0)_{\text{so}} &= 1.32 \text{ fm}, & \lambda &= 36.0 \text{ for protons}, \\ r_0 &= 1.347 \text{ fm}, & (r_0)_{\text{so}} &= 1.31 \text{ fm}, & \lambda &= 35.0 \text{ for neutrons}, \\ V_0 &= 49.6 \text{ MeV}, & a_{\text{ws}} &= 0.70 \text{ fm}, & \kappa &= 0.86, \end{aligned} \quad (2.75)$$

where  $r_0$  and  $(r_0)_{\text{so}}$  are the radius parameters for the central and spin-orbit parts of the potential, respectively.

The pairing interaction strength  $G$ , for BCS approach, Eq. (2.25), is taken in the form of the monopole type with the isotopic dependence:

$$G_l^{\text{BCS}} = (g_{0l} + g_{1l}I)/A. \quad (2.76)$$

The index  $l$  stands for p (protons) or n (neutrons).

The values of the parameters are:

$$\begin{aligned} g_{0l} &= 17.67 \text{ MeV}, \quad g_{1l} = -13.11 \text{ MeV}, \quad \text{for } l = \text{n (neutrons)}, \\ g_{0l} &= 13.40 \text{ MeV}, \quad g_{1l} = 44.89 \text{ MeV}, \quad \text{for } l = \text{p (protons)}. \end{aligned} \quad (2.77)$$

Parameters of the phenomenological formula (2.69) for  $\alpha$ -decay half-lives are:

$$\begin{aligned} a &= 1.5372, \quad b = -0.1607, \quad c = -36.573, \\ \bar{E}_p &= 0.113 \text{ MeV}, \quad \bar{E}_n = 0.171 \text{ MeV}. \end{aligned} \quad (2.78)$$

# Chapter 3

## Results and discussion

### 3.1 One-quasiparticle excitations

We are recently witnessing intensive experimental studies of single-particle structure of heaviest nuclei (e.g. [72–74]). This is connected with a fast progress in synthesis of these nuclei and in detection of their decays. A review of older studies may be found in e.g. [75] and of more recent ones in [29]. Theoretical studies are being also done (e.g. [76–83]).

Experimental identification of spin projections  $\Omega$  and parities  $\pi$  of one-quasiparticle states of odd- $A$  nucleus is rather complicated process. One has to have enough statistics for each state to identify these quantum characteristics. Therefore, theoretical predictions of experimentally unknown as well as description of measured  $\Omega$  and  $\pi$  would be useful for an experimentalist. The goals of the present analysis of single-particle excitations are:

- a) using a macroscopic-microscopic model, without fit of any parameters, to describe known and to calculate experimentally unknown quantum characteristics (spins, parities) and energies of excited states in odd- $A$  nuclei;
- b) to study the sensitivity of the one-particle excitations to changes of the parameters of the model;
- c) taking into account single-particle structure of odd- $A$  nuclei, to analyze decay chains of  $^{269}\text{Ds}$  and  $^{271}\text{Ds}$  and to check, how large are the effects of an odd nucleon in the description of these chains.

Analysis of single-particle excitations was done for odd-proton (with  $Z=93-117$ ,  $N$

is even) and odd-neutron (with  $N=145-161$ ,  $Z$  is even) isotopes. Characteristics of the ground states (g.s.) of the odd- $Z$  nuclei are given in Table 3.1 and for odd- $N$  nuclei in Table 3.2. They are compared with available experimental data which was taken from [27, 28, 31, 33, 84]. Data, which are not certain, are put into round brackets. Also quantum characteristics ( $2\Omega[Nn_z\Lambda]$ ) and excitation energies of 5 lowest proton and neutron excited states are presented in the Tables 3.1 and 3.2. For a shorter notation,  $2\Omega$  is given instead of  $\Omega$ , and parity  $\pi$  of a state has not been shown explicitly, as it is the same as parity of the number  $N$  ( $\pi = (-1)^N$ ).

### 3.1.1 Proton one-quasiparticle states

In most cases, calculated  $\Omega$  and parity agree with experimental ones. More particularly, of 38 cases, in which experimental indications of the values of  $\Omega$  and  $\pi$  are given, the agreement appears in 24 cases (see Table 3.1).

Table 3.1: Ground-state quantum characteristics: theoretical (th) and experimental (exp) given for odd- $Z$  and odd- $A$  nuclei with  $Z=93-117$ , characteristics  $2\Omega[Nn_z\Lambda]$  and excitation energies of the lowest 5 excited states.

$N$	$A$	(exp)	(th)	1	2	3	4	5
–	–	g.s.	g.s.	MeV	MeV	MeV	MeV	MeV
$Z=93$								
136	229	(5)	5[642]	5[523] 0.19	3[521] 0.38	3[651] 0.58	1[530] 1.01	7[514] 1.05
138	231	(5+)	5[642]	5[523] 0.25	3[521] 0.46	3[651] 0.60	1[530] 1.02	1[400] 1.13
140	233	5+	5[642]	5[523] 0.26	3[521] 0.52	3[651] 0.59	1[400] 0.97	1[530] 1.01
142	235	5+	5[642]	5[523] 0.23	3[651] 0.54	3[521] 0.55	1[400] 0.78	1[530] 0.98
144	237	5+	5[642]	5[523] 0.19	3[651] 0.49	3[521] 0.55	1[400] 0.60	3[402] 0.92
146	239	(5+)	5[642]	5[523] 0.13	1[400] 0.41	3[651] 0.43	3[521] 0.52	3[402] 0.73
148	241	(5–)	5[642]	5[523] 0.03	1[400] 0.27	3[651] 0.32	3[521] 0.43	3[402] 0.62
150	243		5[642]	5[523] 0.01	1[400] 0.14	3[651] 0.18	3[521] 0.29	3[402] 0.50
$Z=95$								
140	235		5[523]	5[642] 0.09	3[521] 0.17	7[633] 0.72	3[651] 0.94	7[514] 0.97
142	237	5(–)	5[523]	5[642] 0.10	3[521] 0.18	7[633] 0.66	3[651] 0.91	1[400] 0.98
144	239	(5)–	5[523]	5[642] 0.12	3[521] 0.19	7[633] 0.59	1[400] 0.80	3[651] 0.84
146	241	5–	5[523]	5[642] 0.14	3[521] 0.19	7[633] 0.50	1[400] 0.62	3[651] 0.76

Table 3.1: Cont.

$N$	$A$	(exp)	(th)	1	2	3	4	5
–	–	g.s.	g.s.	MeV	MeV	MeV	MeV	MeV
148	243	5–	5[523]	5[642] 0.07	3[521] 0.14	7[633] 0.42	1[400] 0.45	3[651] 0.59
150	245	(5+)	5[642]	3[521] 0.05	5[523] 0.13	1[400] 0.27	7[633] 0.32	3[651] 0.36
152	247	(5)	3[521]	5[642] 0.01	1[400] 0.13	7[633] 0.22	3[402] 0.22	5[523] 0.30
154	249		3[521]	5[642] 0.02	1[400] 0.12	3[651] 0.19	7[633] 0.20	5[523] 0.41
$Z=97$								
140	237		3[521]	7[633] 0.26	5[523] 0.27	5[642] 0.38	7[514] 0.69	1[521] 0.85
142	239	(7+)	3[521]	7[633] 0.23	5[523] 0.30	5[642] 0.40	7[514] 0.76	1[521] 0.83
144	241	(7+)	3[521]	7[633] 0.18	5[523] 0.31	5[642] 0.43	1[521] 0.81	7[514] 0.84
146	243	(3–)	3[521]	7[633] 0.14	5[523] 0.34	5[642] 0.45	1[521] 0.79	1[400] 0.87
148	245	3–	3[521]	7[633] 0.12	5[642] 0.38	5[523] 0.43	1[400] 0.71	1[521] 0.74
150	247	(3–)	3[521]	7[633] 0.09	5[642] 0.31	1[400] 0.53	5[523] 0.54	1[521] 0.66
152	249	7+	3[521]	7[633] 0.05	5[642] 0.25	1[400] 0.35	3[402] 0.51	1[521] 0.54
154	251	(3–)	3[521]	7[633] 0.03	5[642] 0.20	1[400] 0.30	3[402] 0.44	1[521] 0.47
$Z=99$								
144	243	(7+)	7[633]	3[521] 0.15	1[521] 0.39	7[514] 0.58	5[523] 0.84	5[642] 0.85
146	245	(7+)	7[633]	3[521] 0.14	1[521] 0.37	7[514] 0.66	5[642] 0.85	5[523] 0.86
148	247	(7+)	7[633]	3[521] 0.15	1[521] 0.34	7[514] 0.65	5[642] 0.77	1[400] 0.93
150	249	7+	7[633]	3[521] 0.17	1[521] 0.28	7[514] 0.61	5[642] 0.67	1[400] 0.75
152	251	(3–)	7[633]	3[521] 0.20	1[521] 0.20	1[400] 0.55	5[642] 0.58	7[514] 0.60
154	253	7+	7[633]	1[521] 0.16	3[521] 0.22	1[400] 0.48	7[514] 0.50	5[642] 0.51
156	255	(7+)	7[633]	1[521] 0.12	3[521] 0.25	7[514] 0.38	1[400] 0.40	5[642] 0.43
$Z=101$								
142	243		1[521]	7[514] 0.22	7[633] 0.33	9[624] 0.61	3[521] 0.64	5[512] 0.78
144	245	(7)	1[521]	7[514] 0.24	7[633] 0.36	9[624] 0.62	3[521] 0.64	5[512] 0.81
146	247	(7–)	1[521]	7[514] 0.27	7[633] 0.39	9[624] 0.62	3[521] 0.65	5[512] 0.87
148	249	(7–)	1[521]	7[514] 0.30	7[633] 0.39	9[624] 0.57	3[521] 0.68	5[512] 0.96
150	251	(7–)	1[521]	7[514] 0.30	7[633] 0.37	9[624] 0.49	3[521] 0.70	5[512] 1.03
152	253		1[521]	7[514] 0.32	7[633] 0.36	9[624] 0.43	3[521] 0.72	1[400] 0.88
154	255	(7–)	1[521]	7[514] 0.26	7[633] 0.31	9[624] 0.35	3[521] 0.71	1[400] 0.76
156	257	(7–)	1[521]	7[514] 0.19	7[633] 0.27	9[624] 0.27	1[400] 0.62	3[521] 0.70
158	259	(7–)	1[521]	7[514] 0.09	9[624] 0.20	7[633] 0.22	1[400] 0.53	5[642] 0.67
160	261		7[514]	1[521] 0.01	7[633] 0.14	9[624] 0.16	5[642] 0.49	1[400] 0.55
$Z=103$								

Table 3.1: Cont.

$N$	$A$	(exp)	(th)	1	2	3	4	5
–	–	g.s.	g.s.	MeV	MeV	MeV	MeV	MeV
146	249		7[514]	1[521] 0.06	9[624] 0.18	5[512] 0.44	7[633] 0.70	1[651] 0.88
148	251		7[514]	1[521] 0.08	9[624] 0.13	5[512] 0.50	7[633] 0.72	3[521] 1.04
150	253	(7–)	7[514]	9[624] 0.09	1[521] 0.10	5[512] 0.56	7[633] 0.71	3[521] 1.08
152	255	(7–)	7[514]	9[624] 0.05	1[521] 0.13	5[512] 0.61	7[633] 0.72	3[521] 1.13
154	257	(9+)	7[514]	9[624] 0.04	1[521] 0.13	5[512] 0.62	7[633] 0.65	1[400] 1.02
156	259		7[514]	9[624] 0.02	1[521] 0.13	7[633] 0.58	5[512] 0.62	1[400] 0.86
158	261		7[514]	9[624] 0.01	1[521] 0.10	7[633] 0.50	5[512] 0.56	1[400] 0.74
$Z=105$								
148	253		9[624]	7[514] 0.16	5[512] 0.21	1[521] 0.33	1[651] 1.03	9[505] 1.04
150	255		9[624]	7[514] 0.14	5[512] 0.24	1[521] 0.35	7[633] 1.03	9[505] 1.15
152	257	(9+)	9[624]	7[514] 0.11	5[512] 0.27	1[521] 0.38	7[633] 1.04	9[505] 1.23
154	259		9[624]	7[514] 0.11	5[512] 0.27	1[521] 0.35	7[633] 0.96	1[400] 1.28
156	261		9[624]	7[514] 0.10	5[512] 0.26	1[521] 0.32	7[633] 0.88	1[400] 1.12
158	263		9[624]	7[514] 0.14	5[512] 0.22	1[521] 0.27	7[633] 0.79	1[400] 0.99
$Z=107$								
152	259		5[512]	9[624] 0.48	7[514] 0.75	9[505] 0.92	1[521] 0.94	11[615] 1.02
154	261		5[512]	9[624] 0.54	7[514] 0.80	1[521] 0.96	11[615] 1.04	9[505] 1.11
156	263		5[512]	9[624] 0.59	7[514] 0.85	1[521] 0.95	11[615] 1.05	9[505] 1.23
158	265		5[512]	9[624] 0.62	7[514] 0.88	1[521] 0.92	11[615] 1.05	9[505] 1.33
160	267		5[512]	9[624] 0.53	1[521] 0.72	7[514] 0.94	11[615] 0.96	7[633] 1.33
162	269		5[512]	9[624] 0.44	1[521] 0.54	11[615] 0.84	7[514] 1.01	7[633] 1.16
164	271		5[512]	9[624] 0.35	1[521] 0.38	11[615] 0.67	7[633] 1.02	7[514] 1.08
$Z=109$								
154	263		9[505]	11[615] 0.04	5[512] 0.27	1[651] 0.45	3[512] 0.54	3[642] 0.55
156	265		11[615]	9[505] 0.28	3[512] 0.41	5[512] 0.52	1[510] 0.59	1[651] 0.61
158	267		11[615]	3[512] 0.37	9[505] 0.37	1[510] 0.56	5[512] 0.60	1[651] 0.81
160	269		11[615]	3[512] 0.34	9[505] 0.46	1[510] 0.55	5[512] 0.66	1[651] 0.98
162	271		11[615]	3[512] 0.32	1[510] 0.53	9[505] 0.54	5[512] 0.69	1[521] 1.15
164	273		11[615]	3[512] 0.32	1[510] 0.55	9[505] 0.55	5[512] 0.67	1[521] 0.92
166	275		11[615]	3[512] 0.31	9[505] 0.53	1[510] 0.55	5[512] 0.65	1[521] 0.71
$Z=111$								
160	271		11[615]	3[512] 0.04	9[505] 0.07	1[510] 0.18	1[651] 0.75	3[642] 0.86
162	273		3[512]	11[615] 0.04	1[510] 0.12	9[505] 0.22	1[651] 0.95	5[512] 1.05

Table 3.1: Cont.

$N$	$A$	(exp)	(th)	1	2	3	4	5
–	–	g.s.	g.s.	MeV	MeV	MeV	MeV	MeV
164	275		3[512]	11[615] 0.08	1[510] 0.13	9[505] 0.23	1[521] 1.02	5[512] 1.07
166	277		3[512]	11[615] 0.11	1[510] 0.13	9[505] 0.22	1[521] 0.84	5[512] 1.08
168	279		3[512]	1[510] 0.12	11[615] 0.14	9[505] 0.20	1[521] 0.63	5[512] 1.08
170	281		11[615]	1[521] 0.08	9[505] 0.16	3[512] 0.20	7[503] 0.39	1[510] 0.47
172	283		1[521]	11[615] 0.11	3[512] 0.19	7[503] 0.26	9[505] 0.39	1[510] 0.46
$Z=113$								
164	277		1[510]	3[512] 0.04	9[505] 0.04	11[615] 0.40	7[503] 0.83	1[631] 1.00
166	279		1[510]	9[505] 0.04	3[512] 0.06	11[615] 0.45	7[503] 0.84	1[550] 0.99
168	281		1[510]	9[505] 0.06	3[512] 0.08	11[615] 0.50	1[550] 0.83	7[503] 0.87
170	283		3[512]	1[510] 0.13	7[503] 0.28	1[550] 0.35	9[505] 0.37	11[615] 0.39
172	285		3[512]	1[510] 0.15	7[503] 0.15	1[550] 0.15	11[615] 0.45	13[606] 0.54
174	287		7[503]	1[550] 0.02	3[512] 0.06	13[606] 0.08	1[510] 0.32	11[615] 0.46
176	289		7[503]	1[550] 0.01	3[512] 0.02	13[606] 0.10	1[510] 0.26	11[615] 0.57
$Z=115$								
168	283		1[541]	3[512] 0.35	13[606] 0.59	7[503] 0.62	11[615] 0.65	1[510] 0.71
170	285		1[541]	3[512] 0.27	13[606] 0.39	7[503] 0.45	11[615] 0.56	1[510] 0.61
172	287		1[541]	3[512] 0.16	13[606] 0.29	7[503] 0.38	1[510] 0.49	11[615] 0.63
174	289		1[541]	3[512] 0.06	13[606] 0.16	7[503] 0.29	1[510] 0.36	11[615] 0.75
176	291		1[541]	3[512] 0.11	5[503] 0.43	1[510] 0.53	13[606] 0.69	7[503] 0.71
178	293		1[541]	3[512] 0.11	5[503] 0.22	1[510] 0.58	3[501] 0.78	7[503] 0.88
$Z=117$								
170	287		3[512]	1[510] 0.18	1[541] 0.36	13[606] 0.61	5[503] 0.62	7[503] 0.72
172	289		3[512]	1[510] 0.15	1[541] 0.23	13[606] 0.46	7[503] 0.60	5[503] 0.68
174	291		3[512]	1[510] 0.09	1[541] 0.11	13[606] 0.31	7[503] 0.47	5[503] 0.72
176	293		3[512]	1[541] 0.05	1[510] 0.11	13[606] 0.43	5[503] 0.57	7[503] 0.58
178	295		3[512]	1[541] 0.01	5[503] 0.16	1[510] 0.23	3[501] 0.64	13[606] 1.03

Most of the considered odd- $Z$  nuclei are well deformed. This has been illustrated and discussed in [85] (cf. also the discussion in [86]). Only one nucleus with  $Z=111$ , four nuclei with  $Z=113$  and all nuclei with  $Z=115$  and 117 have  $E_{\text{def}} < 2$  MeV and, thus, are transitional or almost spherical. It means, that the BCS equations may have only trivial

solutions ( $\Delta_p = 0$ ) or BCS pairing energy gap  $\Delta_p$  may be close to zero. Systematics of proton one-quasiparticle excitations for isotopes with  $Z=111$ , 113, 115 and 117 are given in Figs. 3.1-3.4. Generally, larger the excitation energy, stronger is the dependence on  $N$ . In particular, the ground state remains usually the same for a rather long chain of isotopes. Also, we can see from these figures, that for all nuclei proton BCS pairing energy gap  $\Delta_p$  is far from zero. It means, that the use of the BCS approximation for these nuclei is justified.

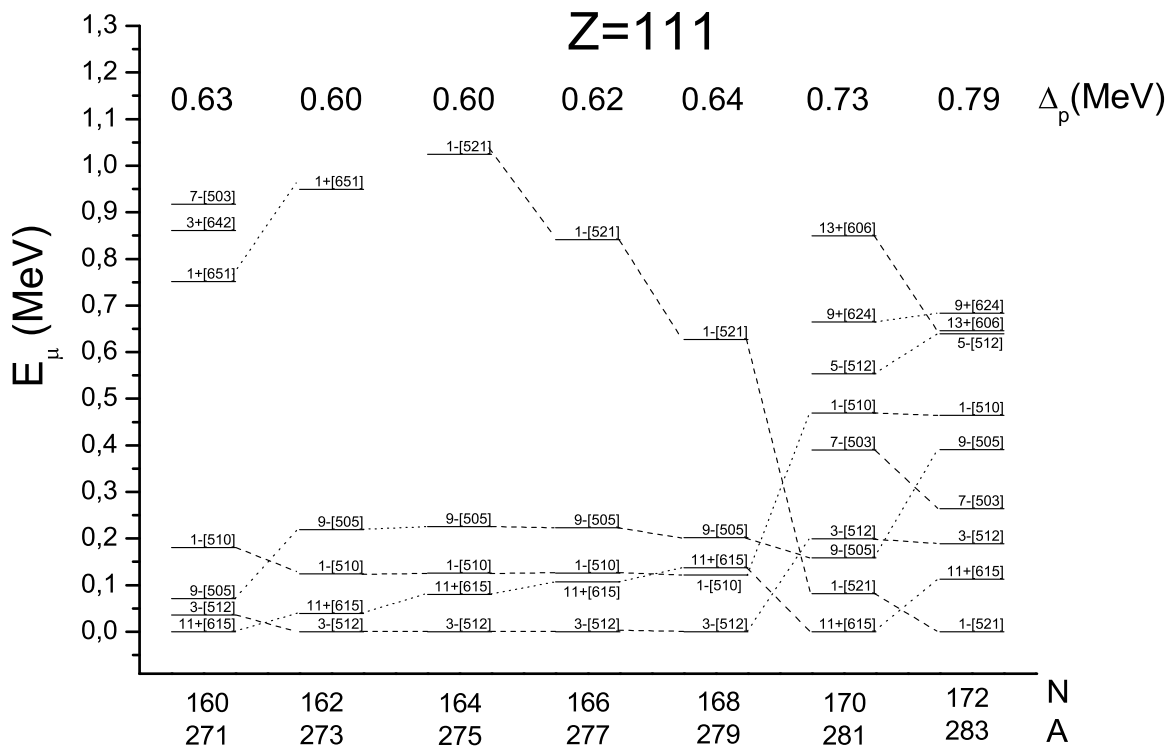


Figure 3.1: Systematics of one-quasiparticle proton states calculated for odd-A isotopes with  $Z=111$ .

Figures 3.5 and 3.6 show a comparison between calculated and measured energies of single-proton states for  $^{241}\text{Am}$  and  $^{237}\text{Np}$ .

For americium, quantum characteristics,  $\Omega$  and  $\pi$ , of the ground states, obtained in experiment, are reproduced by the calculations. The sequence of the excited states is reproduced and the largest difference in the excitation energy is smaller than 300 keV. The one of the worst agreement with an experiment is for  $^{237}\text{Np}$ : the largest discrepancy is about 670 keV, the sequence of the one-quasiparticle energies is not reproduced. Only

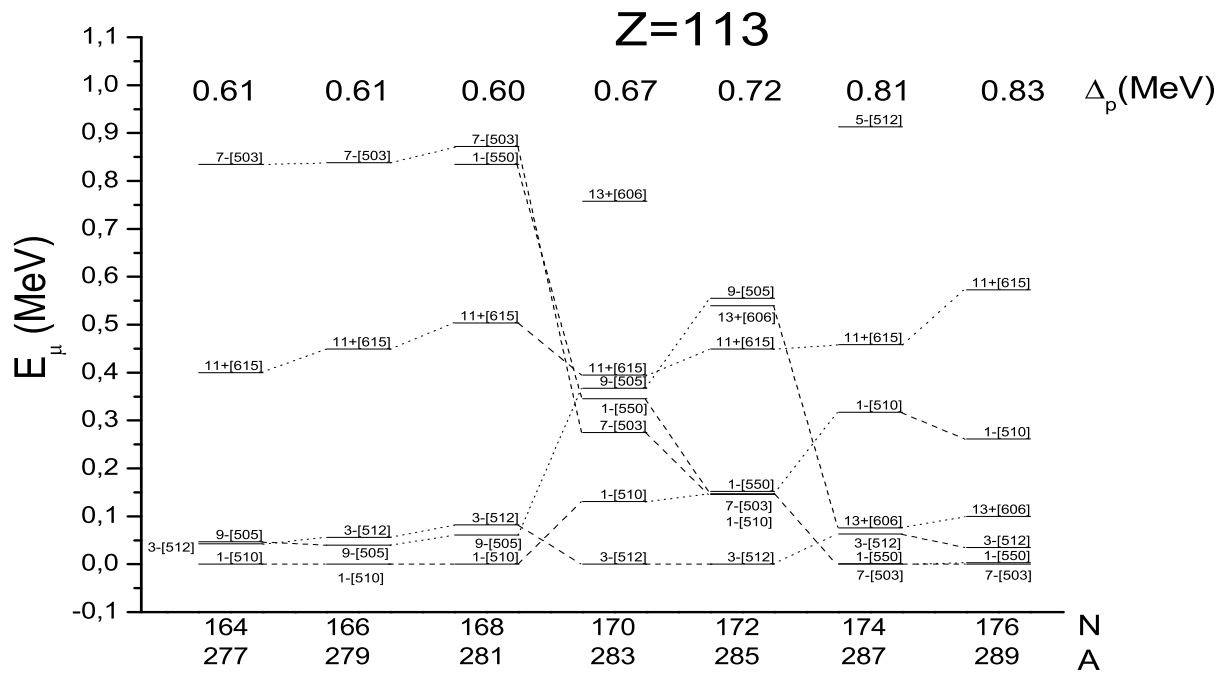


Figure 3.2: Same as in Fig. 3.1, but for the element 113.

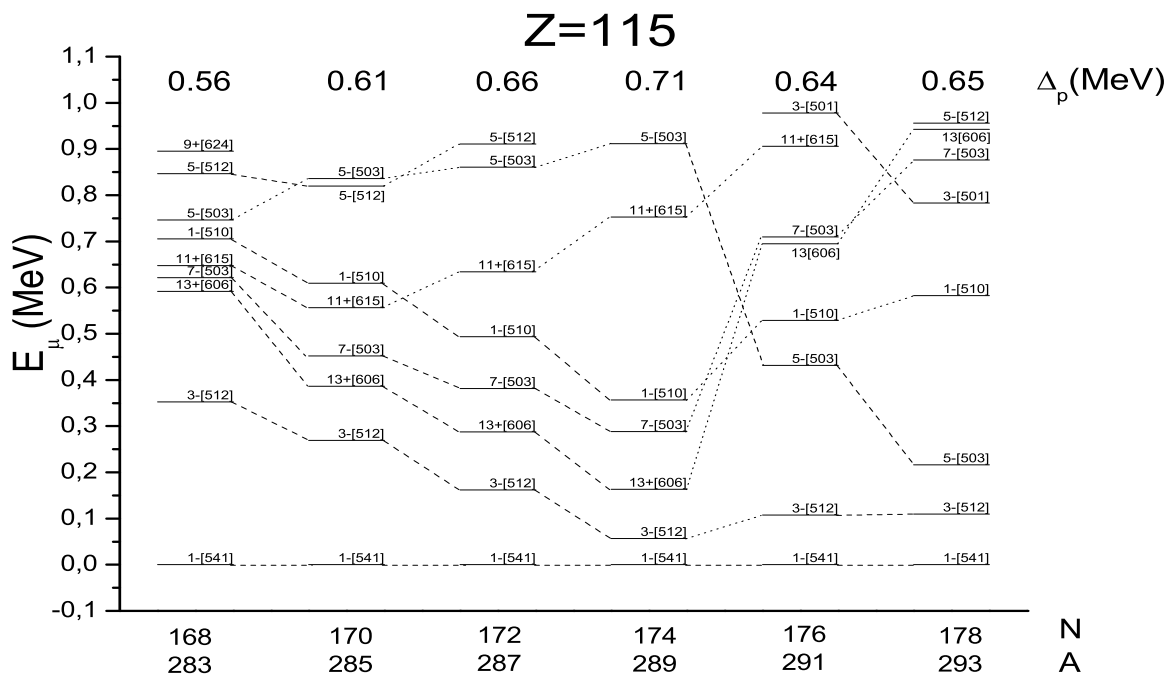


Figure 3.3: Same as in Fig. 3.1, but for the element 115.

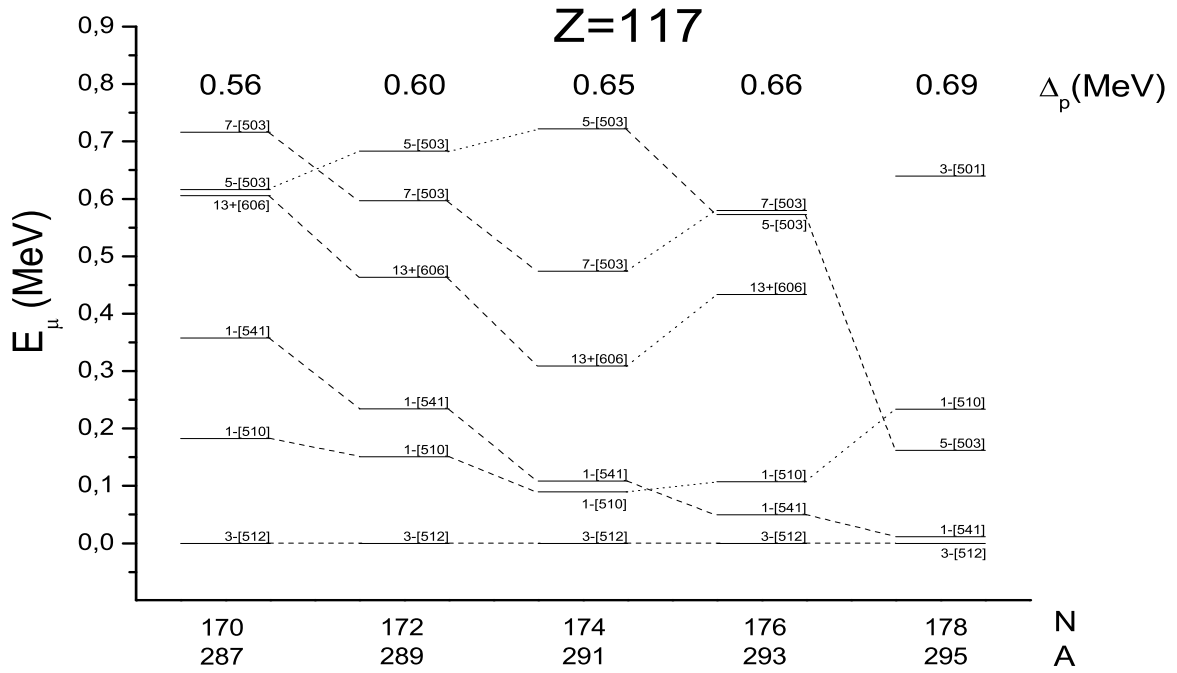


Figure 3.4: Same as in Fig. 3.1, but for the element 117.

spin and parity of the ground state are the same as experimental ones.

The rms, Eq. (5.5), and average discrepancy  $|\overline{\delta E_\mu}|$ , Eq (5.6), for the 4 observed excited states of  $^{241}\text{Am}$  is 151 keV and 111 keV respectively. For 4 levels of  $^{237}\text{Np}$ , rms=369 keV and  $|\overline{\delta E_\mu}|=277$  keV.

Such a comparison of one of the best and one of the worst agreements of the spectra gives us an information about applicability of the model. Experimental values of single-particle states are taken from [84].

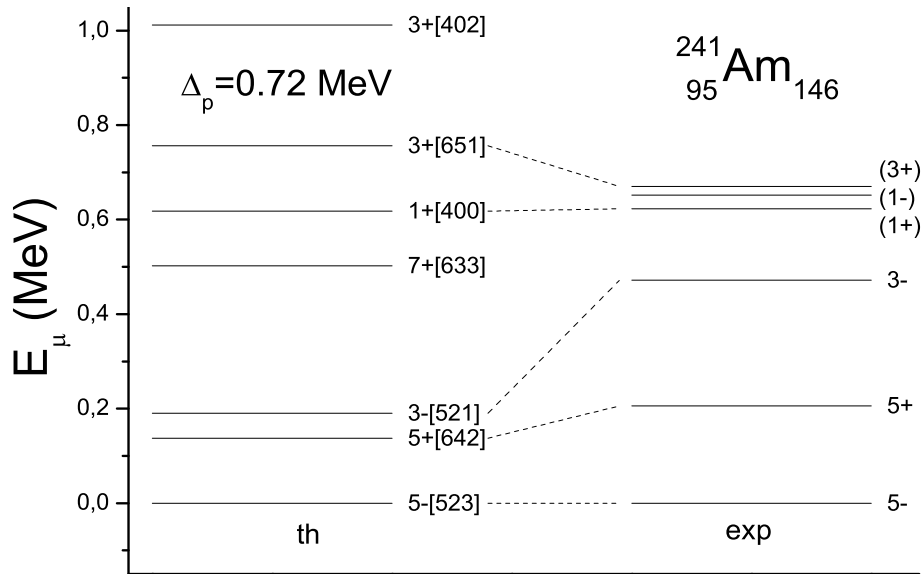


Figure 3.5: Comparison between theoretical and experimental single-proton spectra for the nucleus  $^{241}\text{Am}$ . Data, which are not certain, are put into round brackets

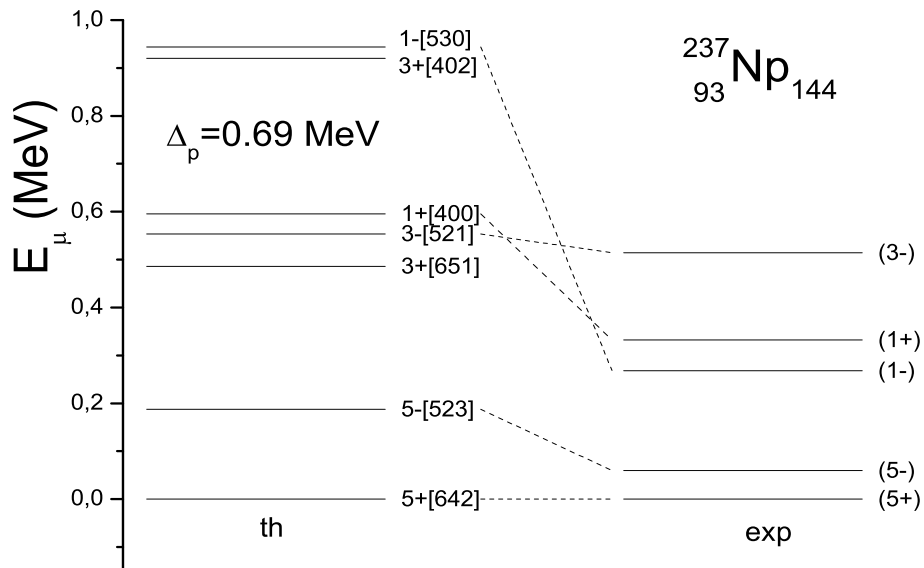


Figure 3.6: The same as in Fig 3.5, but for the nucleus  $^{237}\text{Np}$ .

### 3.1.2 Neutron one-quasiparticle states

As for one-proton excitations, the same analysis was done for one-neutron quasiparticle states. Isotones with  $N=145$  to  $N=161$  were investigated. For neutrons, calculated  $\Omega$  and

parity agree with experimental ones in most cases. More particularly, of 34 cases, in which experimental indications for the values of  $\Omega$  and  $\pi$  are given, the agreement appears in 23 cases. In the rest ones, a calculated state with proper  $\Omega$  and  $\pi$  is often close or even very close in energy to the ground state (e.g.  $^{241}\text{Cm}$ ), but sometimes it is not (e.g.  $^{255}\text{Fm}$ ).

Table 3.2: Quantum characteristics  $2\Omega[\text{Nn}_z\Lambda]$  of the ground state (g.s.) and of five excited states of (even- $Z$ , odd- $N$ ) nuclei with neutron number  $N=145-161$ .

$N$	$A$	(exp)	(th)	1	2	3	4	5
–	–	g.s.	g.s.	MeV	MeV	MeV	MeV	MeV
$N=145$								
90	235	(1+)	7[743]	1[631] 0.05	5[622] 0.12	7[624] 0.53	5[633] 0.57	5[752] 0.71
92	237	1+	7[743]	1[631] 0.04	5[622] 0.14	7[624] 0.57	5[633] 0.58	5[752] 0.77
94	239	1+	7[743]	1[631] 0.02	5[622] 0.16	7[624] 0.59	5[633] 0.62	5[752] 0.81
96	241	1+	7[743]	1[631] 0.00	5[622] 0.14	7[624] 0.52	5[633] 0.67	1[501] 0.69
98	243	(1+)	1[631]	7[743] 0.02	5[622] 0.14	7[624] 0.48	1[501] 0.53	9[734] 0.64
100	245		1[631]	7[743] 0.05	5[622] 0.14	1[501] 0.37	7[624] 0.44	9[734] 0.57
102	247		1[631]	7[743] 0.06	5[622] 0.10	1[501] 0.26	7[624] 0.32	9[734] 0.46
$N=147$								
92	239	5+	5[622]	7[624] 0.26	7[743] 0.26	1[631] 0.34	9[734] 0.47	7[613] 0.93
94	241	5+	5[622]	7[624] 0.25	7[743] 0.30	1[631] 0.34	9[734] 0.43	7[613] 1.00
96	243	5+	5[622]	7[624] 0.21	1[631] 0.31	7[743] 0.32	9[734] 0.37	1[501] 0.99
98	245	5+	5[622]	7[624] 0.17	1[631] 0.30	9[734] 0.31	7[743] 0.34	1[501] 0.81
100	247	(7+)	5[622]	7[624] 0.14	9[734] 0.24	1[631] 0.30	7[743] 0.37	1[501] 0.62
102	249		5[622]	7[624] 0.09	9[734] 0.19	1[631] 0.25	7[743] 0.34	1[501] 0.46
104	251		5[622]	7[624] 0.03	9[734] 0.15	1[631] 0.17	7[743] 0.29	1[501] 0.32
106	253		7[624]	5[622] 0.01	9[734] 0.09	1[631] 0.10	1[501] 0.16	7[743] 0.23
$N=149$								
94	243	7+	7[624]	9[734] 0.10	5[622] 0.10	7[743] 0.50	1[631] 0.54	7[613] 0.71
96	245	7+	7[624]	9[734] 0.08	5[622] 0.10	1[631] 0.53	7[743] 0.53	7[613] 0.80
98	247	(7+)	7[624]	9[734] 0.06	5[622] 0.09	1[631] 0.52	7[743] 0.55	1[620] 0.90
100	249	7+	7[624]	9[734] 0.04	5[622] 0.08	1[631] 0.51	7[743] 0.56	1[501] 0.76
102	251	(7+)	7[624]	9[734] 0.02	5[622] 0.07	1[631] 0.44	7[743] 0.52	1[501] 0.53
104	253		9[734]	7[624] 0.01	5[622] 0.07	1[631] 0.33	1[501] 0.38	7[743] 0.46
106	255		9[734]	7[624] 0.08	5[622] 0.11	1[501] 0.23	1[631] 0.26	7[743] 0.41
$N=151$								

Table 3.2: Cont.

$N$	$A$	(exp)	(th)	1	2	3	4	5
–	–	g.s.	g.s.	MeV	MeV	MeV	MeV	MeV
94	245	(9-)	9[734]	7[624] 0.16	5[622] 0.39	1[620] 0.49	7[613] 0.55	3[622] 0.64
96	247	9-	9[734]	7[624] 0.17	5[622] 0.37	1[620] 0.54	7[613] 0.64	3[622] 0.68
98	249	9-	9[734]	7[624] 0.17	5[622] 0.36	1[620] 0.59	3[622] 0.72	7[613] 0.75
100	251	(9-)	9[734]	7[624] 0.18	5[622] 0.33	1[620] 0.64	3[622] 0.76	1[631] 0.79
102	253	9-	9[734]	7[624] 0.20	5[622] 0.32	1[620] 0.66	1[501] 0.71	1[631] 0.74
104	255	9-	9[734]	7[624] 0.25	5[622] 0.32	1[501] 0.58	1[631] 0.63	1[620] 0.65
106	257		9[734]	7[624] 0.32	5[622] 0.34	1[501] 0.41	1[631] 0.51	1[620] 0.59
$N=153$								
94	247		1[620]	3[622] 0.09	7[613] 0.15	9[734] 0.17	11[725] 0.33	7[624] 0.54
96	249	1(+)	1[620]	3[622] 0.09	7[613] 0.18	9[734] 0.23	11[725] 0.30	7[624] 0.59
98	251	1+	1[620]	3[622] 0.08	7[613] 0.22	11[725] 0.28	9[734] 0.30	7[624] 0.66
100	253	1+	1[620]	3[622] 0.07	11[725] 0.25	7[613] 0.26	9[734] 0.39	9[615] 0.72
102	255	(1+)	1[620]	3[622] 0.06	11[725] 0.22	7[613] 0.37	9[734] 0.47	9[615] 0.82
104	257	1+	1[620]	3[622] 0.06	11[725] 0.15	7[613] 0.36	9[734] 0.48	9[615] 0.75
106	259	(1+)	1[620]	3[622] 0.05	11[725] 0.09	7[613] 0.37	9[734] 0.47	9[615] 0.70
108	261		1[620]	11[725] 0.03	3[622] 0.04	7[613] 0.29	9[734] 0.40	9[615] 0.53
$N=155$								
94	249		1[620]	3[622] 0.02	7[613] 0.06	11[725] 0.14	9[615] 0.39	9[734] 0.46
96	251	(1+)	1[620]	3[622] 0.02	7[613] 0.07	11[725] 0.12	9[615] 0.40	9[734] 0.52
98	253	(7+)	1[620]	3[622] 0.01	11[725] 0.10	7[613] 0.10	9[615] 0.44	9[734] 0.59
100	255	7+	1[620]	3[622] 0.01	11[725] 0.08	7[613] 0.14	9[615] 0.50	9[734] 0.67
102	257	(7+)	1[620]	3[622] 0.00	11[725] 0.05	7[613] 0.20	9[615] 0.55	9[734] 0.73
104	259		1[620]	3[622] 0.00	11[725] 0.03	7[613] 0.21	9[615] 0.51	9[734] 0.74
106	261		1[620]	3[622] 0.00	11[725] 0.01	7[613] 0.22	9[615] 0.48	9[734] 0.74
108	263		1[620]	3[622] 0.00	11[725] 0.00	7[613] 0.18	9[615] 0.35	9[734] 0.69
$N=157$								
96	253		11[725]	7[613] 0.00	3[622] 0.02	1[620] 0.05	9[615] 0.19	9[734] 0.70
98	255	(9+)	11[725]	7[613] 0.02	3[622] 0.03	1[620] 0.07	9[615] 0.24	9[734] 0.80
100	257	(9+)	11[725]	7[613] 0.04	3[622] 0.04	1[620] 0.08	9[615] 0.28	9[734] 0.89
102	259	(9+)	11[725]	3[622] 0.06	7[613] 0.06	1[620] 0.09	9[615] 0.32	9[734] 0.95
104	261		11[725]	3[622] 0.05	7[613] 0.06	1[620] 0.08	9[615] 0.29	9[734] 0.96
106	263		11[725]	3[622] 0.04	7[613] 0.06	1[620] 0.06	9[615] 0.25	9[734] 0.95
108	265		11[725]	3[622] 0.01	7[613] 0.02	1[620] 0.02	9[615] 0.12	9[734] 0.87

Table 3.2: Cont.

$N$	$A$	(exp)	(th)	1	2	3	4	5
–	–	g.s.	g.s.	MeV	MeV	MeV	MeV	MeV
110	267		3[622]	7[613] 0.00	1[620] 0.01	11[725] 0.02	9[615] 0.04	9[734] 0.79
$N=159$								
98	257		9[615]	7[613] 0.00	11[725] 0.03	3[622] 0.11	1[620] 0.16	9[604] 0.82
100	259		7[613]	9[615] 0.05	11[725] 0.08	3[622] 0.19	1[620] 0.24	9[604] 0.94
102	261		7[613]	9[615] 0.04	11[725] 0.11	3[622] 0.20	1[620] 0.24	9[604] 1.08
104	263		7[613]	9[615] 0.04	11[725] 0.15	3[622] 0.23	1[620] 0.27	13[716] 1.17
106	265		7[613]	9[615] 0.05	11[725] 0.21	3[622] 0.28	1[620] 0.31	13[716] 1.21
108	267		7[613]	9[615] 0.01	11[725] 0.19	3[622] 0.19	1[620] 0.21	13[716] 1.10
110	269		9[615]	7[613] 0.01	3[622] 0.11	1[620] 0.12	11[725] 0.16	13[716] 0.95
$N=161$								
100	261		9[615]	7[613] 0.14	11[725] 0.24	3[622] 0.33	1[620] 0.38	13[716] 0.78
102	263		9[615]	7[613] 0.13	11[725] 0.29	3[622] 0.36	1[620] 0.40	13[716] 0.80
104	265		9[615]	7[613] 0.11	11[725] 0.33	3[622] 0.38	1[620] 0.42	13[716] 0.83
106	267		9[615]	7[613] 0.08	11[725] 0.38	3[622] 0.41	1[620] 0.44	13[716] 0.86
108	269		9[615]	7[613] 0.05	3[622] 0.34	11[725] 0.35	1[620] 0.36	13[716] 0.82
110	271		9[615]	7[613] 0.02	3[622] 0.19	1[620] 0.20	11[725] 0.26	13[716] 0.67

Figures 3.7, 3.8 and 3.9 illustrate the dependence of the neutron spectra on proton number  $Z$  (or mass number  $A$ ) for isotones with  $N=151$ , 153 and 161, which are close to  $N=152$  and  $N=162$ , corresponding to neutron deformed shells. Here, all states with the excitation energy up to about 1 MeV are shown. Behaviour of each level with changing  $Z$  as well as of BCS pairing gap  $\Delta_n$  is shown. Generally, larger the excitation energy, stronger is the dependence on  $Z$ .

The pairing-energy gap parameter  $\Delta_n$  is never equal to zero. The smallest value of it (0.36 MeV) is obtained for the nucleus  $^{269}\text{Hs}$ , i.e. the nucleus with the largest shell correction  $E_{\text{sh}}$  [14, 58], which means that it strongly feels the influence of a large energy gap in the neutron single-particle spectrum appearing at the closed deformed shell at  $N=162$ . For such a nucleus, the value  $\Delta_n=0.36$  MeV may be considered as a "normal" value, not influenced by the deficiency of the BCS approximation, appearing at the pairing interaction strength  $G$  close to its critical value  $G_{\text{cr}}$ . A direct check shows that we are

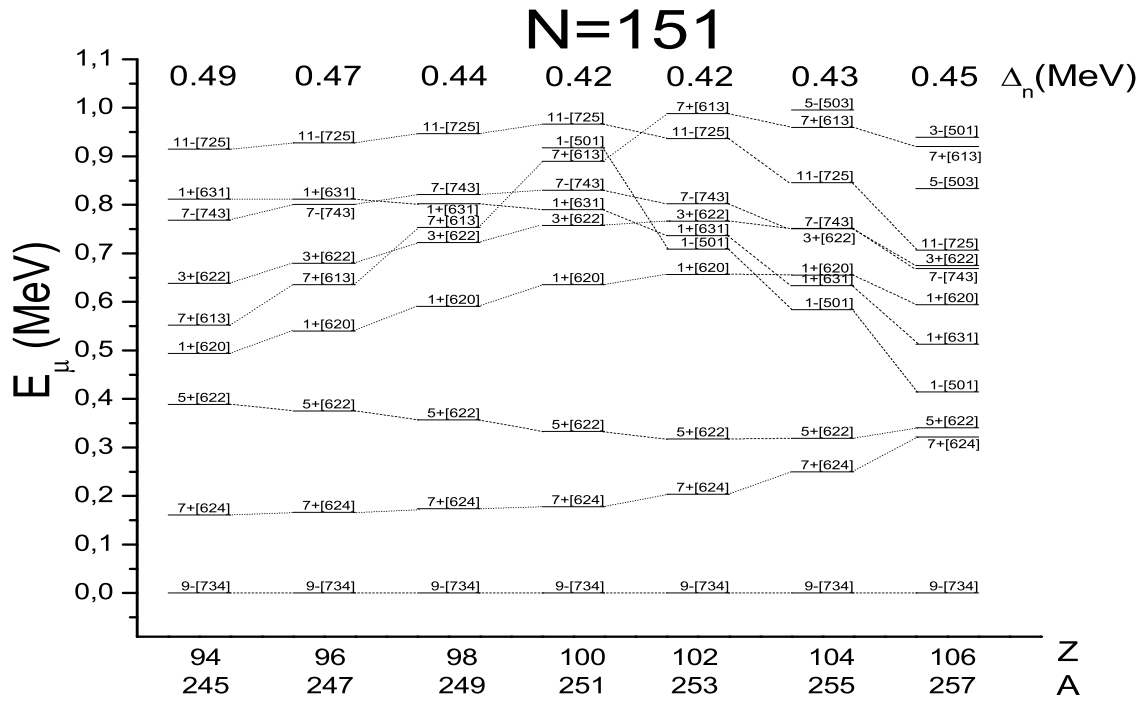


Figure 3.7: Systematics of one-quasiparticle neutron states calculated for odd-A isotones with neutron number  $N=151$ .

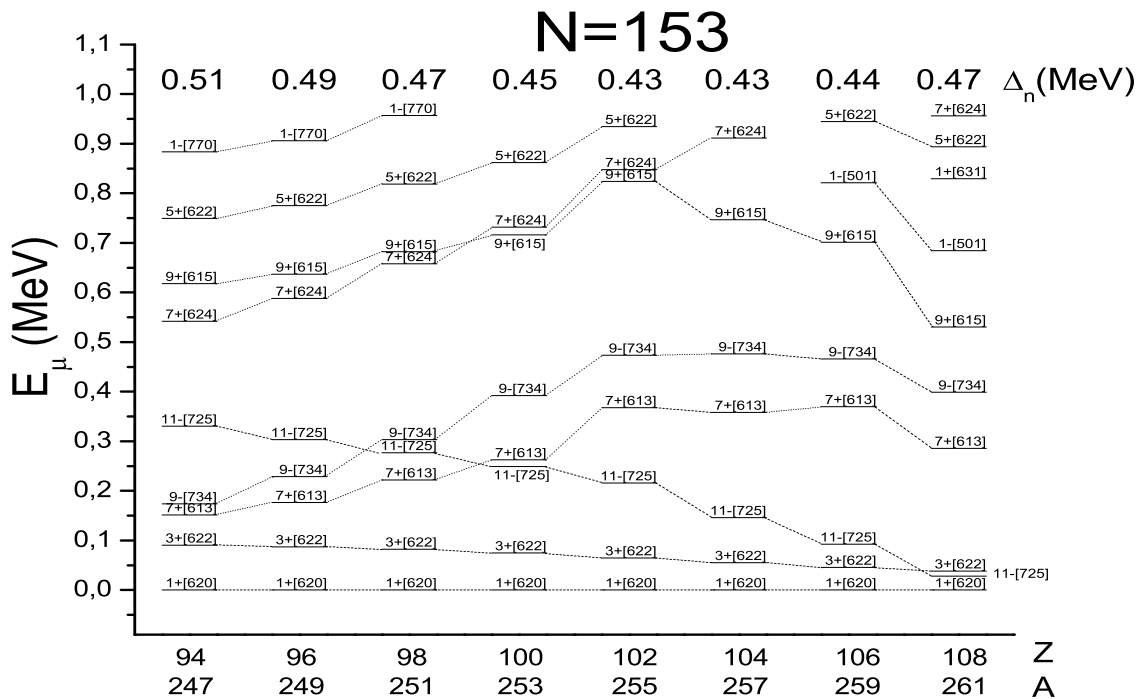


Figure 3.8: Same as in Fig. 3.7, but for  $N=153$ .

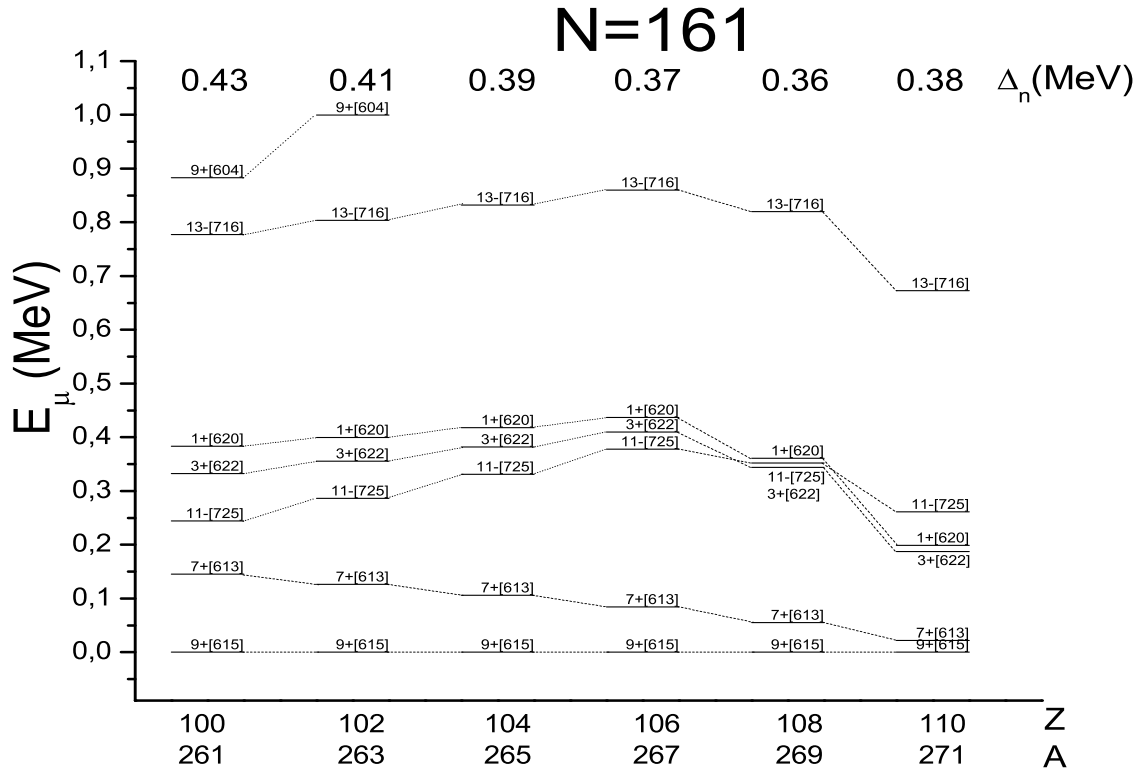


Figure 3.9: Same as in Fig. 3.7, but for  $N=161$ .

really, in this case, in a sufficiently large distance from  $G_{cr}$ .

Comparisons between theoretical and experimental single-neutron excitations of the nuclei  $^{249}\text{Cf}$  and  $^{251}\text{Cf}$  are shown in Figs. 3.10 and 3.11. These nuclei have 151 and 153 neutrons, respectively, and, thus, they are close to the case of the deformed neutron shell at  $N=152$ . For  $^{249}\text{Cf}$ , the discrepancy in energy of the lowest states does not exceed about 300 keV. Average discrepancy  $|\overline{\delta E_\mu}|$ , Eq. (5.6), for the lowest five excited states is 235 keV (rms = 240 keV). For  $^{251}\text{Cf}$ ,  $|\overline{\delta E_\mu}|=73$  keV (rms = 90 keV) for the lowest 6 states. Thus, the discrepancies do not exceed 100 keV. For these two nuclei, the sequences of neutron one-quasiparticle states disagree with experimental ones only for the second and the third levels.

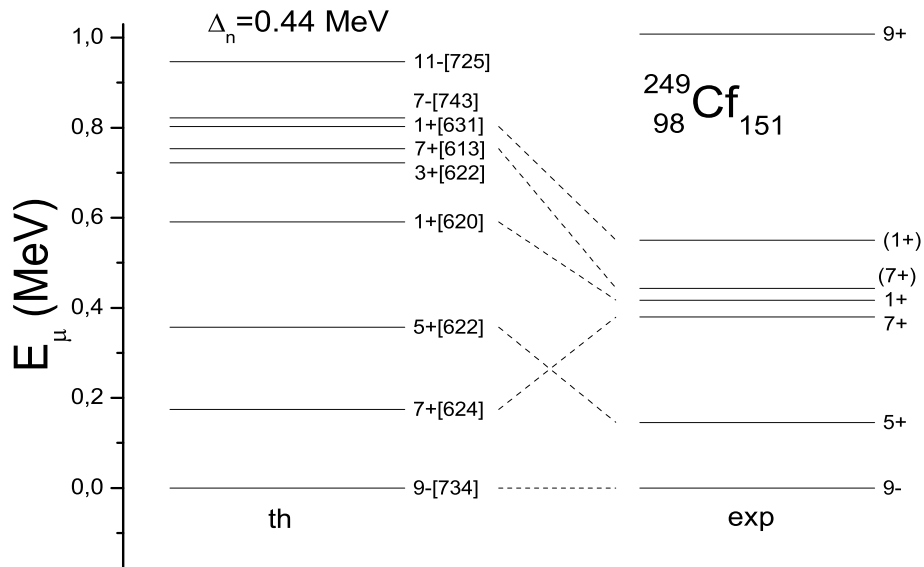


Figure 3.10: Comparison between theoretical and experimental single-neutron excitation spectra for the nucleus  $^{249}\text{Cf}$ .

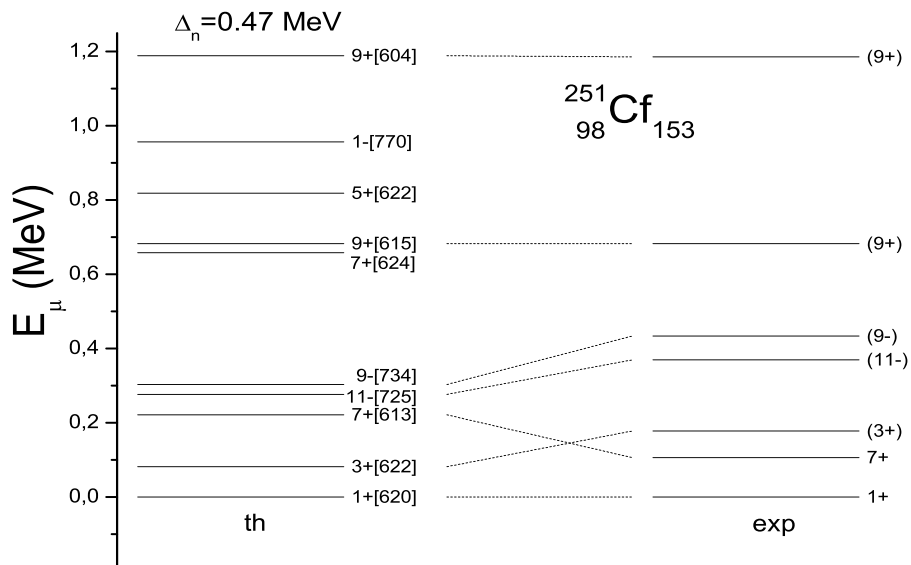


Figure 3.11: The same as in Fig. 3.10, but for the nucleus  $^{251}\text{Cf}$ .

### 3.1.3 Discussion

Figure 3.12, illustrates sensitivity of the calculated one-proton excitation energies to changes of quadrupole deformation:  $\Delta\beta_2 = \pm 0.02$ . One can say that the sensitivity of the exci-

tation energies of single-particle states to changes of such a quantity, as the equilibrium deformation of a nucleus, is rather large. This especially concerns the quadrupole component of the deformation, which should be treated then in the calculations as accurately as possible.

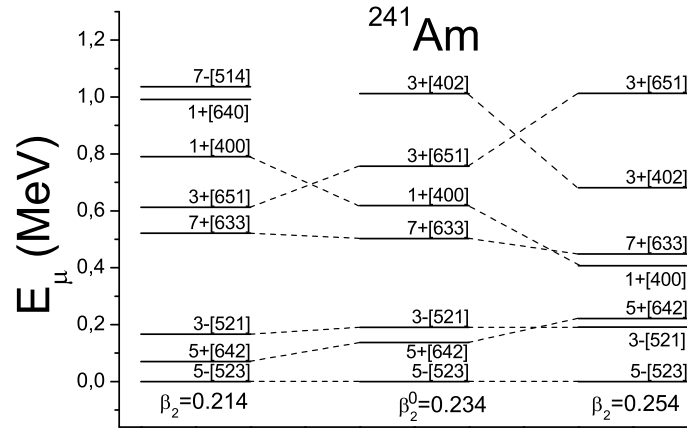


Figure 3.12: Sensitivity of single-proton spectrum of  $^{241}\text{Am}$  to changes of the quadrupole deformation parameter  $\beta_2$ .

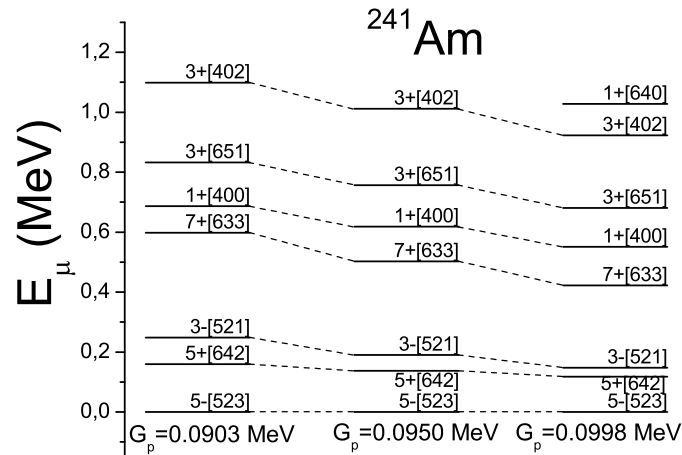


Figure 3.13: The same as in Fig 3.12, but for the proton pairing-interaction strength  $G_p$ .

Sensitivity of the spectrum to changes of the proton pairing-interaction strength  $G_p$  by

$\pm 5\%$  is illustrated in Fig. 3.13. It is clear, that an increase of the strength decreases the excitation energy, making the spectrum more compressed.

Here, the dependencies on pairing interaction strength  $G_p$  and quadrupole deformation  $\beta_2$  are shown only for proton one-quasiparticle levels, since the dependencies of one neutron excitation energies on  $G_n$  and  $\beta_2$  are similar. Discussion of the sensitivity of the proton one-quasiparticle states to changes of  $\beta_4$ ,  $\beta_6$  and  $\beta_8$  can be found in [87].

## 3.2 $\alpha$ -decay half-lives of heaviest nuclei

The aim of this subsection is to illustrate the accuracy of description of  $T_\alpha$  of heavy and superheavy nuclei obtained with the use of a simple phenomenological formula (2.69), found recently [88].

Here, we concentrate on heaviest nuclei with proton number  $Z=84-111$  and neutron number  $N=128-161$ . All kinds of nuclei: even-even (e-e), odd-even (o-e), even-odd (e-o) and odd-odd (o-o) are considered, where e.g. (o-e) means (odd- $Z$ , even- $N$ ) nuclei.

The quality of a phenomenological description of  $T_\alpha$  is analyzed in two cases. The first case is when experimental values of  $Q_\alpha$ ,  $Q_\alpha^{\text{exp}}$ , are taken in the formula (2.69) and the second, when theoretical values  $Q_\alpha^{\text{th}}$  are used.

The first case gives us, as a matter of fact, a check of the quality of the phenomenological formula (2.69), itself. The second one supplies us with a test of the total quality of the calculated  $T_\alpha$ .

Table 3.3 shows averages of absolute values of the quantity

$$\delta \equiv \delta(Z, N) = \log_{10}\{T_\alpha^{\text{ph}}[Q_\alpha(Z, N)]/T_\alpha^{\text{exp}}(Z, N)\}, \quad (3.1)$$

and also rms values for this quantity, for all 4 classes of considered nuclei. Thus,  $\delta$  is the discrepancy between logarithm of calculated (phenomenologically) and measured  $T_\alpha$ , which is equal to logarithm of the ratio of these two values of  $T_\alpha$ , for a given nucleus. In other words,  $\delta$  is the ratio  $T_\alpha^{\text{th}}/T_\alpha^{\text{exp}}$  in the logarithmic scale. The average values of the ratio of calculated and measured  $T_\alpha$ , defined as

$$\bar{f} = 10^{|\bar{\delta}|} \quad (3.2)$$

Table 3.3: Average of  $|\delta|$ , rms values and values of  $\bar{f}$  in the cases when experimental and theoretical values of  $Q_\alpha$  are taken in the calculations.

Nuclei	n	$Q_\alpha = Q_\alpha^{\text{exp}}$			$Q_\alpha = Q_\alpha^{\text{th}}$		
		$ \bar{\delta} $	rms	$\bar{f}$	$ \bar{\delta} $	rms	$\bar{f}$
e-e	61	0.13	0.16	1.3	0.71	0.95	5.1
o-e	45	0.32	0.41	2.1	1.09	1.43	12.3
e-o	55	0.51	0.60	3.2	1.04	1.35	11.0
o-o	40	0.60	0.72	4.0	1.24	1.57	17.4

are also given.

One can see in Table 3.3 that the description of experimental  $T_\alpha$  by calculated values of it is quite good in the case when experimental  $Q_\alpha$  is taken. In the best case of e-e nuclei,  $T_\alpha^{\text{exp}}$  is reproduced by  $T_\alpha^{\text{ph}}$  within an average factor  $\bar{f}=1.3$ , and in the worst case of o-o nuclei, within  $\bar{f}=4.0$ . This means, that the simple 5-parameter formula of Eq. (2.69) appears to be quite good.

One should note here, that when we speak about average factor  $\bar{f}$ , we should remember its definition, Eq. (3.2). The averaging goes here in the logarithmic (and not linear) scale. Averaging of such a quantity as  $f$ , with a rather non-uniform distribution, in linear scale, would make  $\bar{f}$  a very non-informative quantity, making it rather close to  $f_{\text{max}}$ , almost independently of all values, which are much smaller.

In the case, when we use theoretical values of  $Q_\alpha$  in the calculation of  $T_\alpha^{\text{ph}}$ , the accuracy of description of  $T_\alpha^{\text{exp}}$  significantly decreases. As can be seen in Table 3.3, it decreases roughly by a factor of 4.

### 3.2.1 Discussion

#### Quality of the formula

Figure 3.14 gives logarithm of the ratio of the phenomenological half-live  $T_\alpha^{\text{ph}}$ , calculated according to the new formula of Eq. (2.68), to experimental one  $T_\alpha^{\text{exp}}$  for e-e nuclei.

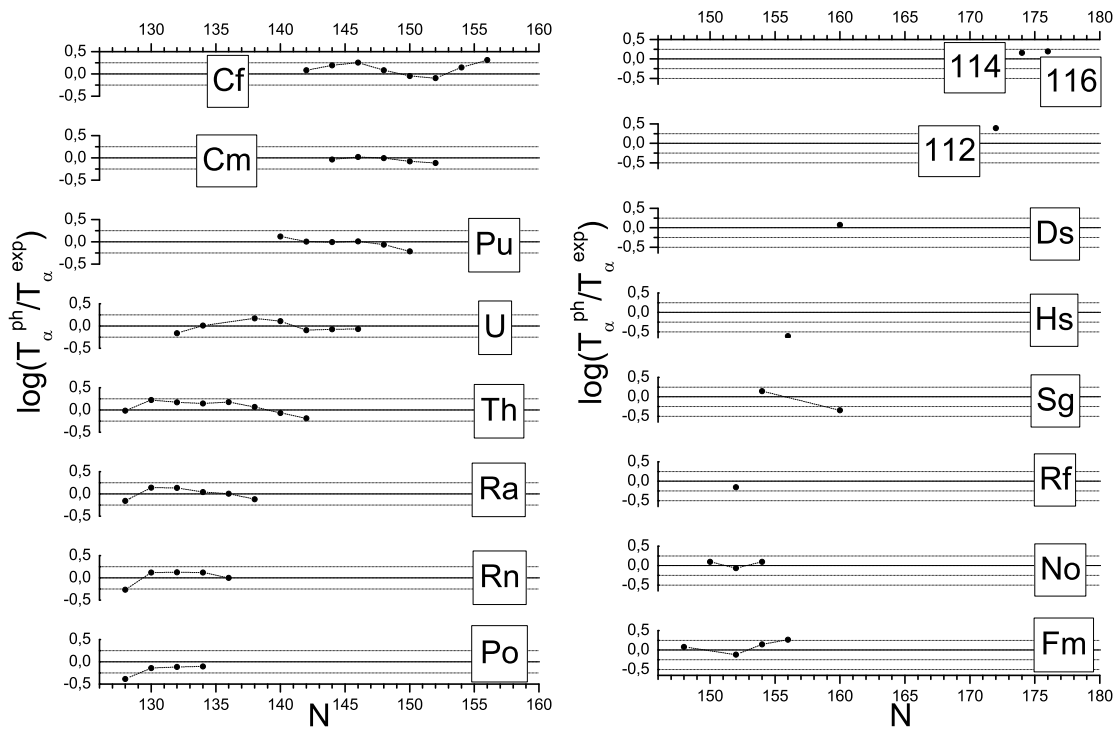


Figure 3.14: Logarithm of the ratio  $T_{\alpha}^{\text{ph}}/T_{\alpha}^{\text{exp}}$  calculated as a function of neutron number  $N$  for even-even nuclei with proton number  $Z=84-116$  [88].

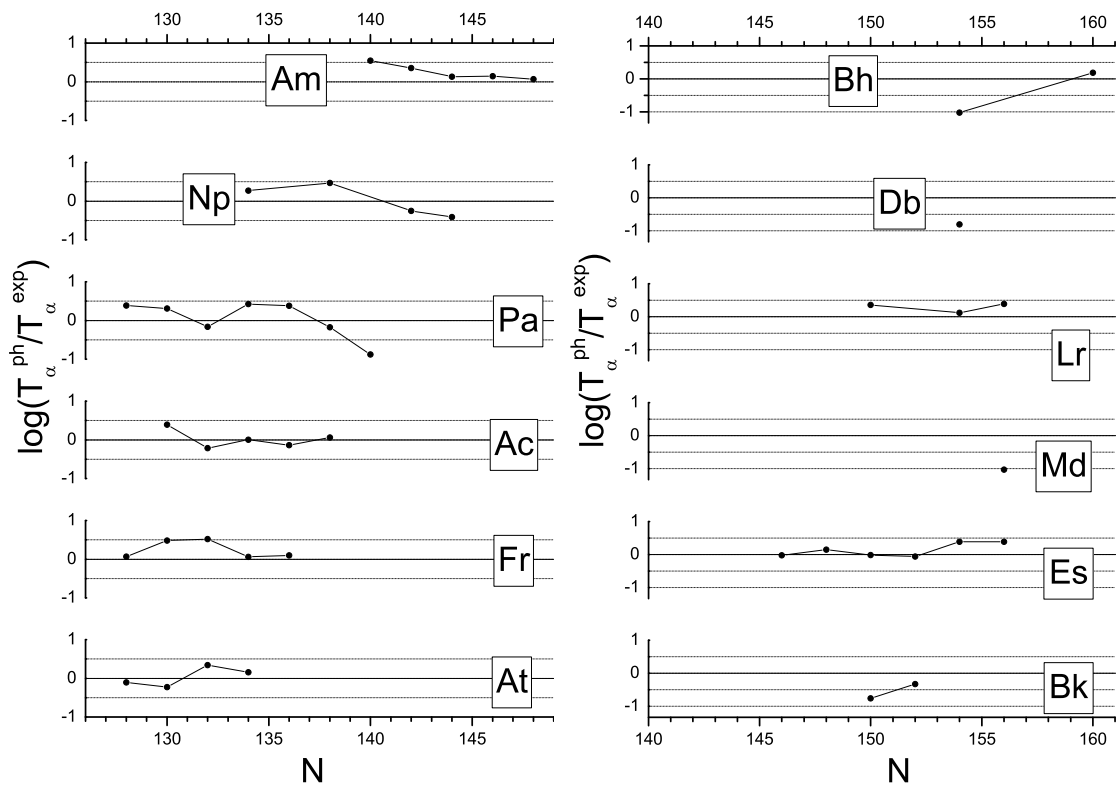


Figure 3.15: Same as in Fig. 3.14, but for odd-even nuclei with  $Z=85-107$  [88].

One can see that, generally, the values are within the range of about  $\pm 0.25$  (which corresponds to the values of the ratio  $T_{\alpha}^{\text{ph}}/T_{\alpha}^{\text{exp}}$  within the range of about 0.56 - 1.78). Only for the nuclei  $^{212}\text{Po}$  and  $^{264}\text{Hs}$ , they are visibly outside this range.

Figure 3.15 illustrates the same quantity as in Fig. 3.14 for o-e nuclei. One can see that here the values of discrepancy are generally within the range of about  $\pm 0.50$  (which corresponds to the values of the ratio  $T_{\alpha}^{\text{ph}}/T_{\alpha}^{\text{exp}}$  within the range of about 0.32 - 3.16). Only for the nuclei  $^{257}\text{Md}$  and  $^{261}\text{Bh}$ , they appear significantly outside this range.

Figure 3.16 shows the discrepancies for e-o nuclei. One can see that they are larger than those for o-e nuclei. For more nuclei, the discrepancies appear outside the range of  $\pm 0.50$ . Especially large discrepancy is obtained for the nucleus  $^{237}\text{Pu}$ .

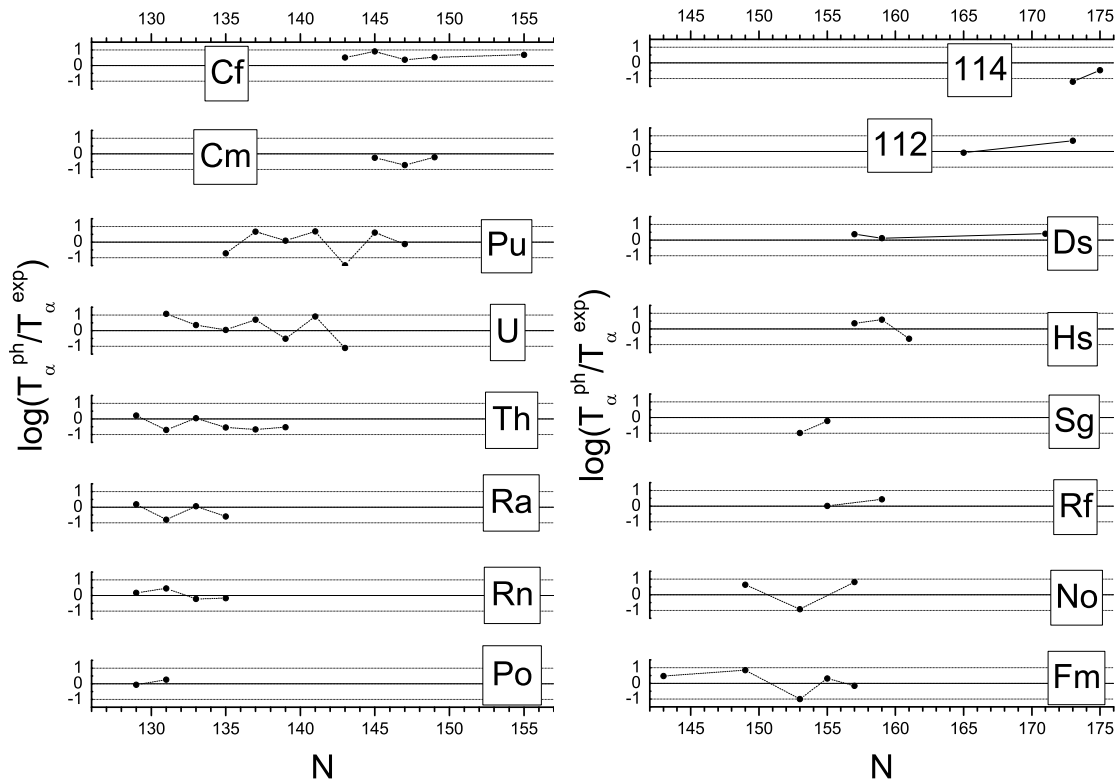


Figure 3.16: Same as in Fig. 3.14, but for even-odd nuclei with  $Z=84-114$  [88].

Finally, Fig. 3.17 presents the discrepancies for o-o nuclei. They are largest among all four classes of nuclei, but not much larger than the discrepancies obtained for e-o nuclei. As for nuclei, for which no adjustable parameters are used, the description of their half-lives

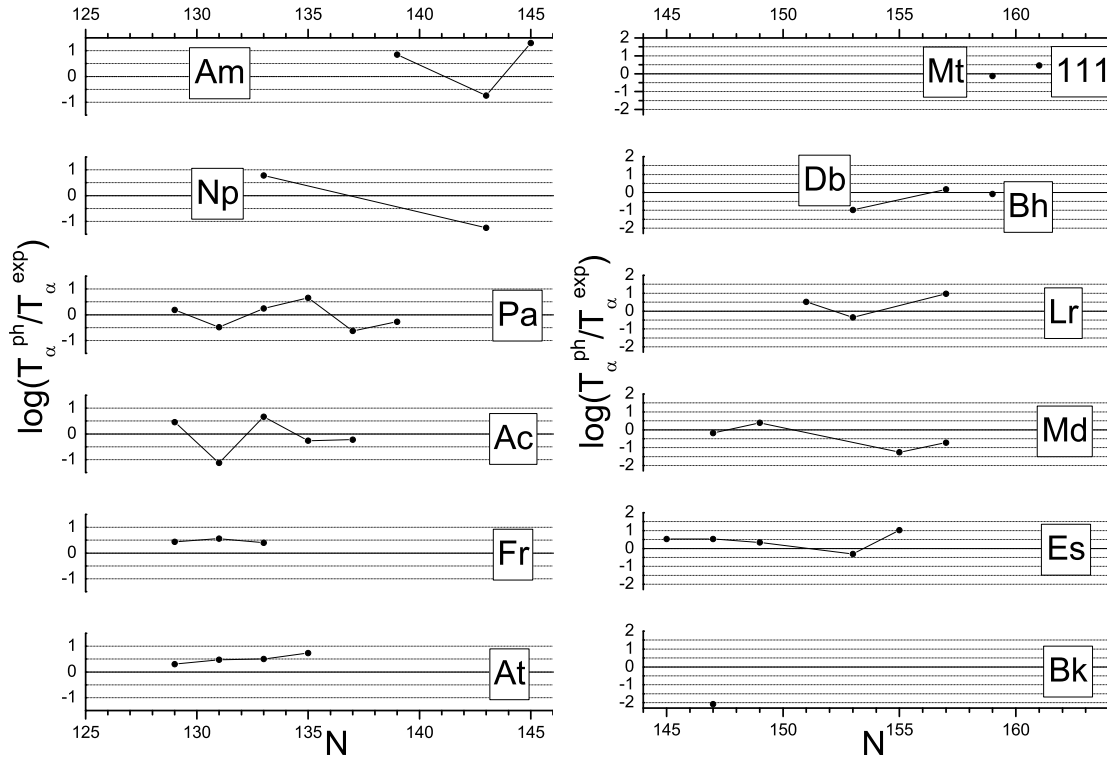


Figure 3.17: Same as in Fig. 3.14, but for odd-odd nuclei with  $Z=85-111$  [88].

is relatively good. The worst case is for  $^{244}\text{Bk}$ , where  $\log(T_\alpha^{\text{ph}}/T_\alpha^{\text{exp}}) \approx -2$ .

Concerning the results presented in Figs. 3.14-3.17, one should add that the parameters of the formula of Eq. (2.69) for  $T_\alpha^{\text{ph}}$  have been fitted only to the data for nuclei with  $Z=84-111$ . Thus, the data for nuclei with  $Z=112-116$ , obtained more recently, may be treated as a test of a predictive power of the formula.

### Effect of electron screening

This effect consists in a smaller kinetic energy of  $\alpha$  particle outside an atom (which is measured) than its energy when it penetrates the Coulomb barrier, due to the orbital electron screening. The screening energy is [89]

$$E_{\text{scr}} = (65.3Z^{7/5} - 80Z^{2/5}) \text{ eV}. \quad (3.3)$$

The energy is rather small. For nuclei from  $^{212}\text{Po}$  to  $^{292}116$ , considered in Fig. 3.14, it changes (smoothly) from 32 keV to 50 keV.

Due to this, its effect on  $T_\alpha$  is also not large, but still significant. The ratio  $\frac{T_\alpha^{\text{ph}}(Q_\alpha^{\text{eff}})}{T_\alpha^{\text{ph}}(Q_\alpha^{\text{exp}})}$ , where

$$Q_\alpha^{\text{eff}} = Q_\alpha^{\text{exp}} + E_{\text{scr}}, \quad (3.4)$$

and  $T_\alpha^{\text{ph}}$  is calculated according to Eq. (2.69), changes within the range from 0.51 to 0.84 for 64 nuclei considered in Fig. 3.14. Thus, the half-life  $T_\alpha^{\text{ph}}$  is reduced by this effect from 16% to 49 % for these nuclei. The magnitude of this relative reduction is correlated with the value of  $Q_\alpha^{\text{exp}}$ . It is lowest for the nucleus  $^{216}\text{Ra}$  with largest  $Q_\alpha^{\text{exp}}$  (9.53 MeV) and is highest for the nucleus  $^{232}\text{Th}$  with smallest  $Q_\alpha^{\text{exp}}$  (4.08 MeV).

It is interesting to see how are the values of the parameters of the new formula, Eq. (2.69), modified by the inclusion of this effect and if the quality of description of  $T_\alpha$  is improved by it.

The results for the parameters are

$$\begin{aligned} a &= 1.5394, \quad b = -0.1610, \quad c = -36.596, \\ \bar{E}_p &= 0.112 \text{ MeV}, \quad \bar{E}_n = 0.171 \text{ MeV}. \end{aligned} \quad (3.5)$$

Table 3.4: Results obtained with the formula of Eq. (2.69) in the case, when the screening effect is taken into account.

Nuclei	N	$ \bar{\delta} $	rms	$\bar{f}$	$n_p$	$\bar{E}$
						MeV
e-e	61	0.128	0.165	1.34	3	0
o-e	45	0.318	0.408	2.08	1	0.112
e-o	55	0.507	0.602	3.21	1	0.171
o-o	40	0.603	0.724	4.01	0	0.283

To get them, we put  $Q_\alpha^{\text{eff}}$  instead of  $Q_\alpha^{\text{exp}}$  in the fitting procedure, i.e. we minimized  $\chi^2$  corresponding to the differences

$$\log_{10} T_\alpha^{\text{exp}}(Z, N) - \{aZ[Q_\alpha^{\text{eff}}(Z, N) - \bar{E}_i]^{-1/2} + bZ + c\}. \quad (3.6)$$

One can see that the obtained values of the parameters, Eq. (3.5), are almost the same as in the case when the effect is not taken into account, Eq. (2.78). The results for the quality of description of  $T_\alpha$  are shown in Table 3.4, where  $n_p$  is number of adjustable parameters.

Comparison of Table 3.4 with Table 3.3 shows that inclusion of the screening effect to the formula of Eq. (2.69) does not improve description of  $T_\alpha$  of considered nuclei.

### Effect of using $\bar{E}_i$ instead of $\bar{h}_i$ as adjustable parameters

To see this effect, we look at the results obtained with the formula

$$\log_{10} T_\alpha^{\text{ph}}(Z, N) = (aZQ_\alpha^{-1/2} + bZ + c) + \bar{h}_i, \quad (3.7)$$

similar to that of Viola and Seaborg, and compare them with the results obtained with the formula of Eq. (2.69). Naturally, the results will be different only for o-e, e-o and o-o nuclei, i.e. for nuclei with one or two odd nucleons. The results are shown in Table 3.5.

Table 3.5: Results obtained with the formula of Eq. (3.7)

Nuclei	N	$ \bar{\delta} $	rms	$\bar{f}$	$n_p$	$\bar{h}_i$
e-e	61	0.128	0.165	1.34	3	0
o-e	45	0.356	0.456	2.27	1	0.433
e-o	55	0.564	0.645	3.66	1	0.643
o-o	40	0.689	0.810	4.89	0	1.076

A comparison between the results of Table 3.3 and those of Table 3.5 shows that the former are better than the latter ones. This is probably because the assumption of about the same excitation energy  $\bar{E}_i$  of a state of a daughter nucleus, which has the same structure as the g.s. of the parent nucleus, is more realistic than the assumption of about the same hindrance factor  $\bar{h}_i$ . This may be argued in the following way. The state with the same characteristics as the g.s. of a parent nucleus should not be far in energy from the g.s. of the daughter nucleus, independently where the nucleus is located in the studied region, especially if the region is not too large. Thus, the assumption of constant  $\bar{E}_i$  inside the

region seems to be realistic. But, effect of this constant  $\bar{E}_i$  on  $T_\alpha$  may be quite different for nuclei with different  $Q_\alpha$ , resulting in different hindrances  $h_i$ . Due to this, the assumption of constant  $h_i$  for a large region of nuclei seems to be less realistic.

### Effect of level density

As density of single-particle levels increases with increasing mass number  $A$  of a nucleus, one might think about modifying, in Eq. (2.69), the expression for the excitation energy of the state to which  $\alpha$  particle goes. As the energy increases (within a simple model of harmonic oscillator) proportionally to  $A^{1/3}$ , one could propose the formula

$$\log_{10} T_\alpha^{\text{ph}}(Z, N) = aZ(Q_\alpha - \bar{E}_i A^{-1/3})^{-1/2} + bZ + c. \quad (3.8)$$

A direct check shows, however, that this does not improve the description of  $T_\alpha$  of heaviest nuclei considered in the present paper.

### 3.3 Interpretation of odd- $A$ $\alpha$ - decay chains

Main information on superheavy nuclei comes from observation of their  $\alpha$ -decay chains (e.g. [35–39,62–64]). Most of these chains have been observed for odd- $A$  nuclei. Figure 3.18 presents heavy and superheavy nuclei that have been synthesized up to the present and most of which belong to such chains. It is important then to see how well these chains can be described theoretically. A number of such tests have been already done (e.g. [76–80]), using various approaches.

For an odd- $A$  nucleus (e-o, o-e), we assume that the decay occurs when the odd nucleon goes to the same single-particle state in daughter nucleus as it occupied in a parent one. Certainly, there are possibilities of  $\alpha$ -transitions with changes of the state. The larger energy of such transition and the less difference between the initial and the final states, the probability of the transition is greater, but here we concentrate on the  $\alpha$ -transitions to the states with the same structure, as initial ones.

The objective of this section is to learn how well an odd- $A$   $\alpha$ -decay chain can be described with a such assumption. In particular, it is aimed to see how much the description of  $\alpha$  energies and  $\alpha$ -decay half-lives, observed in the chain, may be improved by the knowledge of single-particle spectra of nuclei appearing in the chain. The study is done on the example of the even- $Z$ , odd- $N$  nuclei  $^{269}\text{Ds}$  and  $^{271}\text{Ds}$ .

The most natural decay chains of  $^{269}\text{Ds}$  and  $^{271}\text{Ds}$  are presented in Fig 3.19 and 3.20, respectively. The figures are done in a rather unconventional way, when the ground states (g.s.) of all nuclei in the chains are put at the same level. This unconventional presentations have, however, a number of advantages. They better use the space of the pictures, allow one to see directly the excitation energy of single-particle states and to easily compare the spectra of all nuclei with each other. It is also easy to see how much is the transition energy  $Q_\alpha^t$  changed with respect to the  $\alpha$ -decay (g.s. to g.s. transition) energy  $Q_\alpha$  by the odd-particle effect.

Unconventional is also the specification of  $2\Omega$  instead of  $\Omega$  (projection of spin on the symmetry axis of a nucleus) at each energy level, done for a simplification of the notation.



### 3.3.1 $^{269}\text{Ds}$

Spectra of lowest energy levels of nuclei appearing in the  $^{269}\text{Ds}$   $\alpha$ -decay chain are plotted in Fig. 3.19. We show here one of possible interpretations of  $^{269}\text{Ds}$  decay chain, which seems to be the most natural.

The spectra, calculated in [79], are given as a help to interpret the observed [90]  $\alpha$ -decay energies in this chain, i.e. to specify between which states of consecutive nuclei the decay occurs.

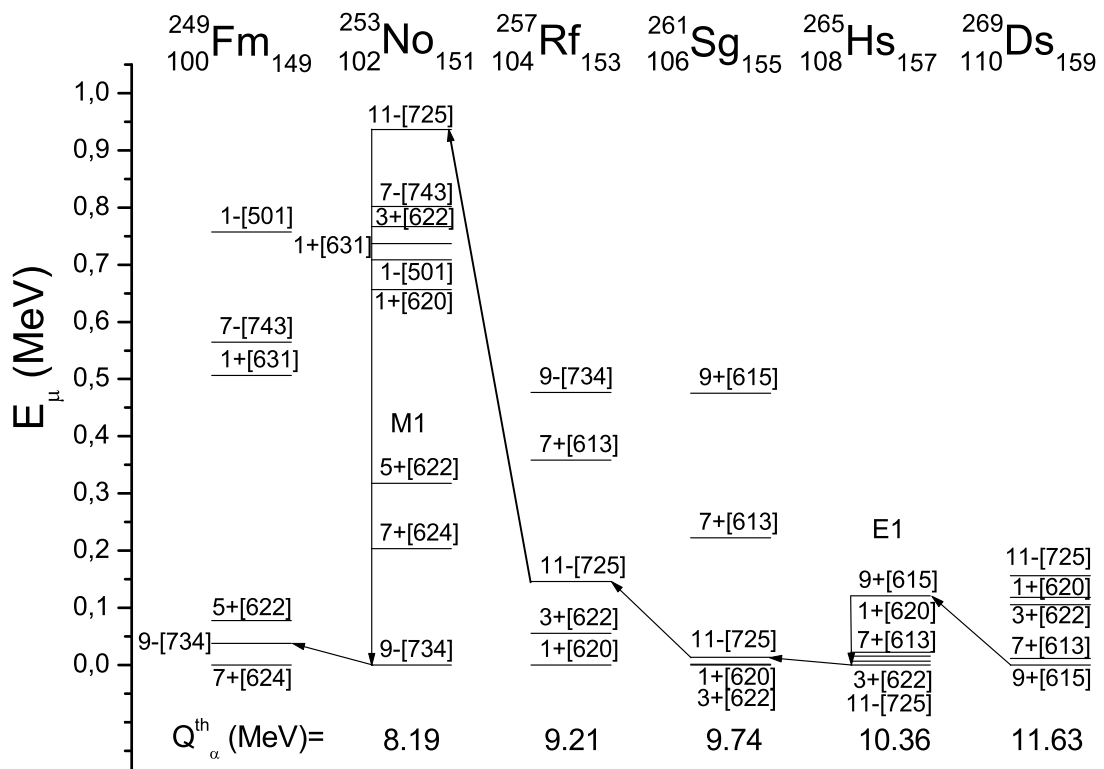


Figure 3.19: Calculated single-particle spectra of nuclei belonging to the  $\alpha$ -decay chain of the nucleus  $^{269}\text{Ds}$ . Assumed sequence of consecutive  $\alpha$  and  $\gamma$  decays is shown by the arrows. Theoretical values of  $\alpha$ -decay energies  $Q_\alpha$  of the nuclei are also shown.

The first transition starts from the g.s.  $9+[615]$  of the nucleus  $^{269}\text{Ds}$  and leads to the excited state  $9+[615]$  of  $^{265}\text{Hs}$ , which undergoes  $\gamma$  decay of the E1 type to the ground state  $11-[725]$ . The second one leads from this state to the isomeric low lying state  $11-[725]$  of  $^{261}\text{Sg}$  and then goes to isomeric one of  $^{257}\text{Rf}$ , from which,  $\alpha$ -decay leads to a highly excited

state 11-[725] of  $^{253}\text{No}$ . After emitting M1 gamma, the nucleus comes to the ground state 9-[734], from which it decays to the excited state 9-[734] of  $^{249}\text{Fm}$ .

Calculated and experimental values of  $\alpha$ -transition energies  $Q_\alpha^t$  (Eq. 2.67) along the described chain, as well as differences between them,  $\delta Q_\alpha^t \equiv Q_\alpha^{t,\text{th}} - Q_\alpha^{t,\text{exp}}$ , are given in Table 3.6. Theoretical values of  $\alpha$ -decay energies  $Q_\alpha$  (g.s. to g.s. transitions) and the contribution  $\Delta E \equiv Q_\alpha^t - Q_\alpha$  of quasiparticle excitation energies to the  $\alpha$ -transition energies are also given. Theoretical values of  $Q_\alpha$ ,  $Q_\alpha^{\text{th}}$ , are taken from [60,61]. Experimental values  $Q_\alpha^{t,\text{exp}}$  is taken from [61], where they were deduced from the data of [90].

Table 3.6: Values of the quantities characteristic for the decay chain of  $^{269}\text{Ds}$ .

Nucleus	$Q_\alpha^{t,\text{th}}$	$Q_\alpha^{t,\text{exp}}$	$\delta Q_\alpha^t$	$Q_\alpha^{\text{th}}$	$\Delta E$	$T_\alpha^{\text{th}}$	$T_\alpha^{\text{exp}}$	$f$
-	MeV	MeV	MeV	MeV	MeV			
$^{269}\text{Ds}$	11.51	11.28	0.23	11.63	-0.12	40 $\mu\text{s}$	179 $\mu\text{s}$	4.5
$^{265}\text{Hs}$	10.35	10.72	-0.37	10.36	-0.01	4.7 ms	701 $\mu\text{s}$	6.7
$^{261}\text{Sg}$	9.60	9.68	-0.08	9.74	-0.14	96 ms	61 ms	1.6
$^{257}\text{Rf}$	8.42	8.80	-0.38	9.21	-0.79	64 s	9.4 s	6.8
$^{253}\text{No}$	8.15	8.21	-0.06	8.19	-0.04	90.8 s	92.4 s	1.0

One can see in the figure and in the table that the effect of odd nucleon is large. The effect  $\Delta E$  changes from -790 keV to about zero, along the studied chain. It is especially large in the decay of  $^{257}\text{Rf}$  to  $^{253}\text{No}$ .

Alpha-decay half-lives  $T_\alpha$  are calculated according to the formula (2.68). One can see that the calculated values reproduce experimental ones within a factor  $f$  ( $f \equiv T_\alpha^{\text{th}}/T_\alpha^{\text{exp}}$  or  $T_\alpha^{\text{exp}}/T_\alpha^{\text{th}}$ ), which is smaller than 7. The average value of  $f$  for the 5 transitions is 4.2, and average discrepancy  $|\overline{\delta Q_\alpha^t}|=0.22$  MeV. As no adjustable parameter is used, the result may be considered as good. Also the agreement between  $Q_\alpha^{t,\text{th}}$  and  $Q_\alpha^{t,\text{exp}}$  is reasonable.

### 3.3.2 $^{271}\text{Ds}$

Figure 3.20 shows spectra of lowest energy levels of nuclei appearing in the  $\alpha$ -decay chain of the nucleus  $^{271}\text{Ds}$  and indicates the decay path, which seems to be the most natural.

According to it, the first transition starts from the g.s.  $9+[615]$  of the nucleus  $^{271}\text{Ds}$  and leads to the low excited state  $9+[615]$  of  $^{267}\text{Hs}$ . This state decays by gamma emission of the E1 type to the g.s.  $7+[613]$ . The second  $\alpha$ -decay leads from this state to the low excited state  $7+[613]$  of  $^{263}\text{Sg}$ , which undergoes  $\gamma$  decay of the E2 type to a lower state  $3+[622]$ . From this state, the third  $\alpha$  transition leads to a very low state  $3+[622]$  of  $^{259}\text{Rf}$ . We assume that this state decays by gamma emission of the M1 type to the g.s.  $1+[620]$ , from which, the last  $\alpha$ -transition leads to the g.s. state  $1+[620]$  of  $^{255}\text{No}$ .

Numerical values of quantities connected with the chain are given in Table 3.7. Theoretical values of  $Q_\alpha$ ,  $Q_\alpha^{\text{th}}$ , are taken from [60, 61]. Experimental values  $Q_\alpha^{\text{t,exp}}$  is taken from [61], where they were deduced from the data of [38, 39].

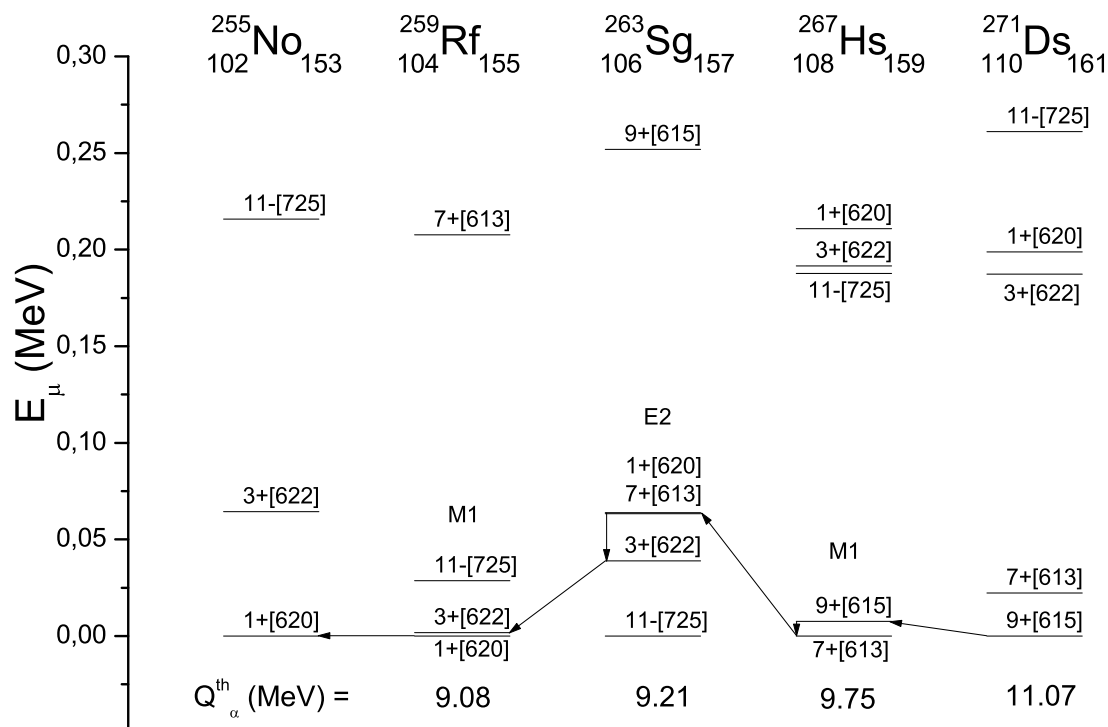


Figure 3.20: Same as in Fig. 3.19, but for the decay chain of the nucleus  $^{271}\text{Ds}$ .

One can see in Table 3.7 that measured  $\alpha$ -transition energies  $Q_\alpha^{\text{t,exp}}$  are described with

an average discrepancy  $|\overline{\delta Q_\alpha^t}|=0.17$  MeV. The discrepancy for all four decays does not exceed 0.34 MeV. The contribution of single-particle effects  $\Delta E$  to  $Q_\alpha^t$  is small, it does not exceed 0.06 MeV in absolute value. Description of observed half-lives is also rather good. The ratio  $f$  of the larger value of  $Q_\alpha^{\text{th}}$  and  $Q_\alpha^{\text{exp}}$  to the smaller one does not exceed 5.2 and the average of this ratio for all four transitions is 3.8.

Table 3.7: The same as in Table 3.6 but for the decay chain of the nucleus  $^{271}\text{Ds}$ .

Nucleus	$Q_\alpha^{\text{t,th}}$	$Q_\alpha^{\text{t,exp}}$	$\delta Q_\alpha^{\text{t}}$	$Q_\alpha^{\text{th}}$	$\Delta E$	$T_\alpha^{\text{th}}$	$T_\alpha^{\text{exp}}$	$f$
-	MeV	MeV	MeV	MeV	MeV			
$^{271}\text{Ds}$	11.06	10.91	0.15	11.07	-0.01	0.39 ms	1.1 ms	2.8
$^{267}\text{Hs}$	9.69	10.03	-0.34	9.75	-0.06	0.25 s	59 ms	4.2
$^{263}\text{Sg}$	9.25	9.39	-0.14	9.21	0.04	0.93 s	0.31 s	3.0
$^{259}\text{Rf}$	9.08	9.03	0.05	9.08	0.00	0.59 s	3.1 s	5.3

We considered here the most natural interpretation of the observed decay chain of  $^{271}\text{Ds}$ . One could certainly admit another one. For example, as the state  $3+[622]$  of  $^{259}\text{Rf}$  has very low (calculated) energy, 2 keV, one can assume that the transition from it goes directly by  $\alpha$  emission to the excited state  $3+[622]$  of  $^{255}\text{No}$ , instead of  $\gamma$  transition of the M1 type to the g.s.  $1+[620]$  of  $^{259}\text{Rf}$  and only then to g.s.  $1+[620]$  of  $^{255}\text{No}$  by  $\gamma$  emission. In such a case  $Q_\alpha^{\text{t,th}}$  for the decay  $^{259}\text{Rf}$  would be 9.02 MeV (instead of 9.08 MeV) and  $T_\alpha^{\text{th}}$  would be 0.88 s (instead of 0.59 s). Thus the agreement with measured values of  $Q_\alpha^{\text{t}}$  and  $T_\alpha$  would be even better.

# Chapter 4

## Conclusions

Our study may be summarized and concluded in the following way:

1. For all of investigated proton-odd and neutron-odd nuclei, pairing energy strength  $G$  is larger than its critical value  $G_{cr}$  and distant from it. Due to this, the BCS approximation, used in the paper, is justified (the smallest value of the pairing gap parameter is  $\Delta_n = 0.36$  MeV, obtained for the nucleus  $^{269}\text{Hs}$ ).
2. Quantum characteristics of most of the experimentally known ground states of analyzed here odd-A nuclei are reproduced by the calculations. More particularly, this happens for 24 of 38 odd-proton and for 23 of 34 odd-neutron nuclei.
3. Excitation energy of known lowest single-particle states is reproduced by the applied model within the average accuracy of about 200 keV.
4. The Nilsson label (asymptotic harmonic oscillator (h.o.) quantum numbers) of a given nuclear single-particle state is quite representative for the structure of this state, even if the contribution of the asymptotic h.o. state to the given state is not large. This means that if two given states, in two different nuclei, have the same Nilsson label, the next h.o. components of the given states are usually the same and with similar contributions to these states. At least, as far as three main components (analyzed in [79]) are concerned.

5. Sensitivity of single-particle excitation energies to changes of such a quantity as the equilibrium deformation of a nucleus is rather large. This especially concerns the quadrupole component of the deformation, which should be then treated in the calculations as accurately as possible. Also there is a strong dependence of these energies on the pairing interaction strength for both protons and neutrons.

6. A new, simple phenomenological formula proposed for description of the  $\alpha$ -decay half-lives  $T_\alpha(Q_\alpha)$  of heaviest e-e, o-e, e-o and o-o nuclei uses only 5 adjustable parameters: 3 to describe e-e nuclei and 2 for description of nuclei with odd proton and odd neutron, one for each. (As the role of an odd nucleon in  $T_\alpha$  is important, we consider such a separation of the roles of adjustable parameters as also significant). The formula allows one to describe  $T_\alpha^{\text{exp}}$  of 61 e-e nuclei roughly within a factor of 1.3, 45 o-e nuclei within a factor of 2.1, 55 e-o nuclei within a factor of 3.2 and 40 o-o nuclei within a factor of 4.0, on the average, when  $Q_\alpha^{\text{exp}}$  is taken. In the analysis, 201 nuclei with proton number  $Z=84-111$  and neutron number  $N=128-161$ , with measured values of both  $Q_\alpha$  and  $T_\alpha$ , are taken.

7. The accuracy of the mentioned above phenomenological formula decreases by a factor of about 4, when theoretical values of  $Q_\alpha^{\text{th}}$ , instead of experimental ones  $Q_\alpha^{\text{exp}}$ , are used. The theoretical values  $Q_\alpha^{\text{th}}$  are obtained within a macroscopic-microscopic approach and reproduce the experimental values of  $Q_\alpha$  of the same nuclei with an average accuracy of about 190 keV for even-even, 270 keV for odd-even, 260 keV for even-odd and 330 keV for odd-odd nuclei.

8. It is found that description of the decay chains of  $^{269}\text{Ds}$  and  $^{271}\text{Ds}$  is rather good. The absolute values of the discrepancies for the transition energy  $Q_\alpha^{\text{t}}$  do not exceed 0.38 MeV and 0.34 MeV, respectively. The ratio  $f$  of the larger value of  $T_\alpha^{\text{th}}$  and  $T_\alpha^{\text{exp}}$  to the smaller one does not exceed 6.8 for the  $^{269}\text{Ds}$  and 5.3 for the  $^{271}\text{Ds}$  chains. No free parameters have been used in the description.

# Acknowledgements

First of all I would like to thank my supervisor Prof. Adam Sobiczewski for directing my Ph.D. work and his support during my stay at the Sołtan Institute for Nuclear Studies.

I would also like to thank the director of the Institute, Prof. Ziemowid Sujkowski, the scientific secretary, Dr Danuta Chmielewska, the director of the Ph.D. Studies at the Institute, Prof. Leszek Łukaszuk, the secretary of these Studies, Mgr Tomasz Papuziński and the secretary of P-VIII Department, Mrs. Anna Sidor, for their support.

Support by the Polish State Committee for Scientific Research (KBN), grants no. 2 P03B 039 22 and 1 P03B 042 30, as well as the Polish-JINR (Dubna) Cooperation Programme is gratefully acknowledged.

My special thanks goes to my parents and to my family. I own a lot to my wife for her patience, love, support and friendship.

Acknowledgements are due to my friends Igor Muntian, Michał Kowal, Leonid Shvedov, Oleg and Nina Utyuzh, Aliaksandr Bantsar, Paulina Chojnacka, Andriy Mikulyak, Dmytro Melnichuk, Aneta Gójska, Sergiy Mezhevich, Viktor Trubnikov for helpful discussions and support.



# Chapter 5

## Appendix

### 5.1 Least-square method

Suppose that we are fitting  $N$  data points  $(x_\mu, y_\mu)$   $\mu = 1, \dots, N$ , to a model that has  $M$  adjustable parameters  $a_j, j = 1, \dots, M$ . The model predicts a functional relationship between the measured independent and dependent variables,

$$y(x) = y(x; a_1, \dots, a_M), \quad (5.1)$$

where the dependence on the parameters is indicated explicitly on the right-hand side. What, exactly, do we want to minimize to get fitted values for the  $a_j$ 's? The first thing that comes to mind is the familiar least-squares fit,

$$\text{minimize over } a_1, \dots, a_M : \sum_{\mu=1}^N [y_\mu - y(x_\mu; a_1, \dots, a_M)]^2. \quad (5.2)$$

But what general principles is it based on? The answer to these questions takes us into the subject of *maximum likelihood estimators*. Given a particular data set of  $x_\mu$ 's and  $y_\mu$ 's, we have the intuitive feeling that some parameter sets  $a_1 \dots a_M$  are very unlikely those for which the model function  $y(x)$  looks nothing like the data – while others may be very likely – those that closely resemble the data. How can we quantify this intuitive feeling? How can we select fitted parameters that are "most likely" to be correct? It is not meaningful to ask the question: "What is the probability that a particular set of fitted parameters  $a_1 \dots a_M$  is correct?" The reason is that there is no statistical universe of

models from which the parameters are drawn. There is just one model, the correct one, and a statistical universe of data sets that are drawn from it!

That being the case, we can, however, turn the question around, and ask, "Given a particular set of parameters, what is the probability that this data set could have occurred?" If the probability of obtaining the data set is infinitesimally small, then we can conclude that the parameters under consideration are "unlikely" to be right. Conversely, our intuition tells us that the data set should not be too improbable for the correct choice of parameters. In other words, we identify the probability of the data given the parameters (which is a mathematically computable number), as the likelihood of the parameters given the data. This identification is entirely based on intuition. It has no formal mathematical basis in and of itself. Once we make this intuitive identification, however, it is only a small further step to decide to fit for the parameters  $a_1 \dots a_M$  precisely by finding those values that maximize the likelihood defined in the above way. This form of parameter estimation is maximum likelihood estimation. We are now ready to make the connection to Eq. (5.2). Suppose that each data point  $y_\mu$  has a measurement error that is independently random and distributed as a normal (Gaussian) distribution around the "true" model  $y(x)$ . In other words this mean that the differences between a theoretical and experimental values of some quantity are normally distributed. And suppose that the standard deviations  $\sigma$  of these normal distributions are the same for all points. Then the probability of the data set, or experimentally measured values is the product of the probabilities of each point,

$$P \propto \prod_{\mu=1}^N \left\{ \exp \left[ -\frac{1}{2} \left( \frac{y_\mu - y(x_\mu)}{\sigma} \right)^2 \right] \right\}. \quad (5.3)$$

Maximizing Eq. (5.4) is equivalent to maximizing its logarithm, or minimizing the negative of its logarithm, namely,

$$\sum_{\mu=1}^N \frac{[y_\mu - y(x_\mu)]^2}{\sigma}. \quad (5.4)$$

Since  $\sigma$  is a constant, minimizing this equation is equivalent to minimizing Eq. (5.2). What we see is that least-squares fitting is a maximum likelihood estimation of the fitted parameters if the measurement errors are independent and normally distributed with constant standard deviation.

All model parameters in this work were fitted using this method. In the dissertation, quality of the description of the physical quantity  $y$  is characterized by root-mean-square, rms, and average discrepancy,  $|\overline{\delta y_\mu}|$ :

$$\text{rms} = \sqrt{\frac{\sum_{\mu=1}^N [y_\mu - y(x_\mu)]^2}{N}}, \quad (5.5)$$

$$|\overline{\delta y_\mu}| = \frac{1}{N} \sum_{\mu=1}^N |y_\mu - y(x_\mu)|, \quad (5.6)$$

where  $y_\mu$  and  $y(x_\mu)$  are respectively observed (experimental) and theoretical values of physical quantity.

## 5.2 Probabilities of $\alpha$ -decays and $\gamma$ -decays

To find a way which  $\alpha$ -decay chain goes with our assumptions ( $\alpha$ -decays in the chain occur when the odd nucleon goes to the same single-particle state in daughter nucleus as it occupied in a parent one), we have to know if the considered excited single-particle state is isomeric or not. If it is, then  $\alpha$ -decay occurs from this state to the state with the same structure in a daughter nucleus; if it is not, then  $\gamma$ -decay takes place to one of the lower states in a parent nucleus and then this state is investigated in the way described above.

To identify such an isomeric state, probability of  $\alpha$ -decay of the nucleus from this state to a state of the daughter nucleus has been compared with the largest probability of all probabilities of  $\gamma$ -decay from this state to lower levels (Fig 5.1). If  $\alpha$ -decay probability is greater, than this state is considered as isomeric.

### 5.2.1 Estimating the probabilities of $\alpha$ -decay

Let us consider a collection of the same (with the same number of protons and neutrons)  $N$  nuclei, which emits  $\alpha$ -particles. Probability  $\lambda$  of  $\alpha$ -decay per unit time is a constant for this kind of nuclei, such, that during time  $dt$ ,  $\lambda N dt$  nuclei decay, on the average:

$$dN = -\lambda N dt, \quad (5.7)$$

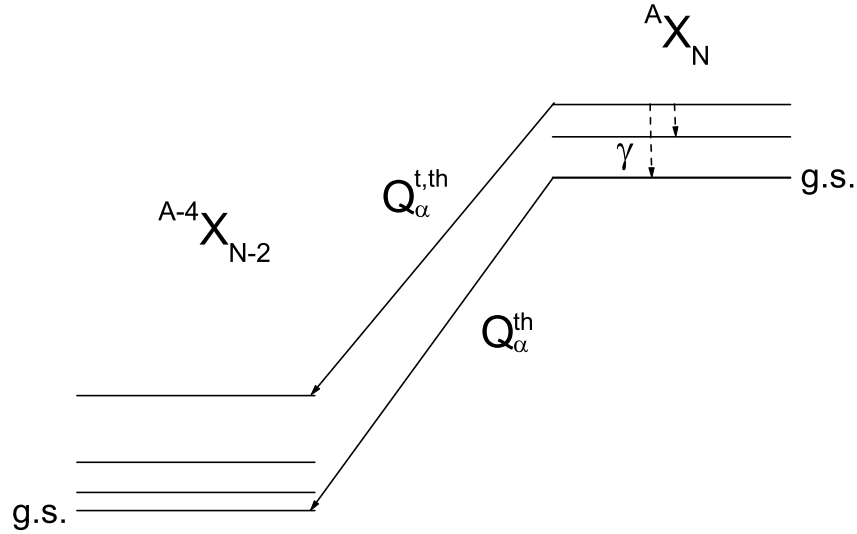


Figure 5.1: Schematic illustration of most general situation of  $\alpha$ -decay: parent nucleus decays from isomeric state to excited state of a daughter nucleus.  $Q_{\alpha}^{th}$  corresponds to g.s. to g.s. transition,  $Q_{\alpha}^{t,th}$  includes single-particle structure of decaying and daughter nuclei.

where the sign minus means, that number of  $\alpha$ -emitters is decreasing. After integrating Eq. (5.7), we have:

$$N = N_0 e^{-\lambda t}, \quad (5.8)$$

where  $N_0$  is the number of  $\alpha$ -radioactive nuclei at the beginning. Alpha-decay half-life  $T_{1/2}$  (in this work it has been used  $T_{\alpha}$  instead of  $T_{1/2}$ ) is the time, in which decays a half of nuclei:

$$N_0/2 = N_0 e^{-\lambda T_{\alpha}}, \quad (5.9)$$

or

$$\lambda = \ln 2 / T_{\alpha}. \quad (5.10)$$

Equations (5.7)-(5.10), definitions of  $\lambda$  and  $T_{1/2}$  are useful, of course, not only for  $\alpha$ -decay, but for all types of radioactive decay.

For odd- $A$  nuclei, using formula

$$\log_{10} T_{\alpha} = \frac{aZ}{\sqrt{Q_{\alpha}^{\text{t,th}}}} + bZ + c, \quad (5.11)$$

with calculated  $Q_{\alpha}^{\text{t,th}} = Q_{\alpha}^{\text{th}} + (E_{\text{p}}^{\text{th}} - E_{\text{d}}^{\text{th}})$  and Eq. (5.10),  $\alpha$ -decay probabilities were obtained for all nuclei in  $\alpha$ -decay chains of  $^{269}\text{Ds}$  and  $^{271}\text{Ds}$ . The quantities  $E_{\text{p}}^{\text{th}}$  and  $E_{\text{d}}^{\text{th}}$  are theoretical one-quasiparticle excitation energies of initial (parent nucleus) and final (daughter nucleus), respectively.

### 5.2.2 Estimating the probabilities of $\gamma$ -decay

Table 5.1 gives the transition probabilities  $T_{fi}$  and the Weisskopf units for the the  $B(\lambda)$  values in the most probable cases, that were used in this work to estimate the probabilities of  $\gamma$ -decay.

Table 5.1: Transition probabilities  $T$  ( $\text{sec}^{-1}$ ) expressed by  $B(EI)$  and  $B(MI)$ , and the Weisskopf units  $B_{sp}$  expressed in  $(e^2(fm)^{2I})$  and  $\mu_N^2(fm)^{2I-2}$ . Energies  $E$  are measured in MeV.

$T(E1) = 1.587 \cdot 10^{15} \cdot E^3 \cdot B(E1)$	$B_{sp}(E1) = 6.446 \cdot 10^{-2} \cdot A^{2/3}$
$T(E2) = 1.223 \cdot 10^9 \cdot E^5 \cdot B(E2)$	$B_{sp}(E2) = 5.940 \cdot 10^{-2} \cdot A^{4/3}$
$T(E3) = 5.698 \cdot 10^2 \cdot E^7 \cdot B(E3)$	$B_{sp}(E3) = 5.940 \cdot 10^{-2} \cdot A^2$
$T(E4) = 1.694 \cdot 10^{-4} \cdot E^9 \cdot B(E4)$	$B_{sp}(E4) = 6.285 \cdot 10^{-2} \cdot A^{8/3}$
$T(E5) = 3.451 \cdot 10^{-11} \cdot E^{11} \cdot B(E5)$	$B_{sp}(E5) = 6.928 \cdot 10^{-2} \cdot A^{10/3}$
$T(M1) = 1.779 \cdot 10^{13} \cdot E^3 \cdot B(M1)$	$B_{sp}(M1) = 1.790$
$T(M2) = 1.371 \cdot 10^7 \cdot E^5 \cdot B(M2)$	$B_{sp}(M2) = 1.650 \cdot A^{2/3}$
$T(M3) = 6.387 \cdot 10^0 \cdot E^7 \cdot B(M3)$	$B_{sp}(M3) = 1.650 \cdot A^{4/3}$
$T(M4) = 1.899 \cdot 10^{-6} \cdot E^9 \cdot B(M4)$	$B_{sp}(M4) = 1.746 \cdot A^2$
$T(M5) = 3.868 \cdot 10^{-13} \cdot E^{11} \cdot B(M5)$	$B_{sp}(M5) = 1.924 \cdot A^{8/3}$

From Table 5.1 we find that the radiation with higher  $I$ -values is strongly suppressed. Usually, we have to take into account only the lowest possible  $I$ -value. Magnetic radiation

is weaker than the electric one. Therefore, we often have a competition between  $M1$  and  $E2$  radiation. It is also becomes clear that the transition probability  $T$  increases rapidly with the transition energy. This is the reason why transitions with small energy differences are sometimes harder to observe.

# Bibliography

- [1] P. Armbruster, *Ann. Rev. Nucl. Part. Sci.* **35** (1985) 135.
- [2] P. Armbruster, *Proc. Int. School on heavy ion physics*, Erice (Italy) 1986, eds. R.A. Broglia and G.F. Bertsch (Plenum, New York, 1988) 153.
- [3] R. Smolańczuk, J. Skalski and A. Sobiczewski, *Phys. Rev. C* **52** (1995) 1871.
- [4] W.D. Myers and W.J. Swiatecki, *Nucl. Phys.* **81** (1966) 1.
- [5] A. Sobiczewski, F.A. Gareev and B.N. Kalinkin, *Phys. Lett.* **22** (1966) 500.
- [6] H. Meldner, *Ark. Fys.* **36** (1967) 593.
- [7] U. Mosel and W. Greiner, *Z. Phys.* **222** (1969) 261.
- [8] S.G. Nilsson, J.R. Nix, A. Sobiczewski, Z. Szymański, S. Wycech, C. Gustafson and P. Möller, *Nucl. Phys. A* **115** (1968) 545.
- [9] S.G. Nilsson, C.F. Tsang, A. Sobiczewski, Z. Szymański, S. Wycech, C. Gustafson, I.L. Lamm and B. Nilsson, *Nucl. Phys. A* **131** (1969) 1.
- [10] E.O. Fiset and J.R. Nix, *Nucl. Phys. A* **193** (1972) 647.
- [11] M. Brack, J. Damgaard, A.S. Jensen, H.C. Pauli, V.M. Strutinsky, and C.Y. Wong, *Rev. Mod. Phys.* **44** (1972) 320.
- [12] Z. Patyk, A. Sobiczewski, P. Armbruster and K.-H. Schmidt, *Nucl. Phys. A* **491** (1989) 267.
- [13] K. Böning, Z. Patyk, A. Sobiczewski and S. Ćwiok, *Z. Phys. A* **325** (1986) 479.

- 
- [14] Z. Patyk and A. Sobiczewski, *Nucl. Phys. A* **533** (1991) 132.
- [15] Z. Patyk and A. Sobiczewski, *Phys. Lett. B* **256** (1991) 307.
- [16] S. Ówiok, V.V. Pashkevich, J. Dudek and W. Nazarewicz, *Nucl. Phys. A* **410** (1983) 254.
- [17] P. Möller, G.A. Leander and J.R. Nix, *Z. Phys. A* **323** (1986) 41.
- [18] J. Randrup, S.E. Larsson, P.Möller, S.G. Nilsson, K. Pomorski and A. Sobiczewski, *Phys. Rev. C* **13** (1976) 229.
- [19] A. Baran, K. Pomorski, A. Łukasiak and A. Sobiczewski, *Nucl. Phys. A* **361** (1981) 83.
- [20] Z. Łojewski and A. Baran, *Z. Phys. A* **329** (1988) 161.
- [21] Z. Patyk, J. Skalski, A. Sobiczewski and S. Ówiok, *Nucl. Phys. A* **502** (1989) 591c.
- [22] S. Ówiok and A. Sobiczewski, *Z. Phys. A* **342** (1992) 203.
- [23] Z. Patyk, J. Skalski, R.A. Gherghescu and A. Sobiczewski, APH N.S., *Heavy Ion Physics* **7** (1998) 13.
- [24] Z. Łojewski and A. Staszczak, *Acta Phys. Pol. B* **27** (1996) 531.
- [25] Z. Łojewski and A. Staszczak, *Nucl. Phys. A* **657** (1999) 134.
- [26] K. Pomorski and J. Dudek, *Phys. Rev. C* **67** (2003) 044316.
- [27] I. Ahmad, R.R. Chasman and P.R. Fields, *Phys. Rev. C* **61** (2000) 044301.
- [28] F.P. Hessberger, S. Hofmann, D. Ackermann, V. Ninov, M. Leino, G. Münzenberg, S. Saro, A. Lavrentev, A.G. Popeko, A.V. Yeremin and Ch. Stodel, *Eur. Phys. J. A* **12** (2001) 57.
- [29] R.-D. Herzberg, *J. Phys. G* **30** (2004) R123.

- [30] F.P. Hessberger, S. Hofmann, V. Ninov, P. Armbruster, H. Folger, G. Münzenberg, H.J. Schött, A.G. Popeko, A.V. Yeremin, A.N. Andreyev and S. Saro, *Z. Phys. A* **359** (1997) 415.
- [31] F.P. Hessberger, S. Hofmann, D. Ackermann, S. Antalic, P. Cagarda, I. Kojouharov, P. Kuusiniemi, R. Mann and S. Saro, *GSI Sci. Report 2003* (GSI 2004-1, Darmstadt, 2004) 3.
- [32] F.P. Hessberger, S. Hofmann, D. Ackermann, P. Cagarda, R.-D. Herzberg, I. Kojouharov, P. Kuusiniemi, M. Leino and R. Mann, *ibid.*, p. 4.
- [33] F.P. Hessberger, S. Hofmann, D. Ackermann, P. Cagarda, R.-D. Herzberg, I. Kojouharov, P. Kuusiniemi, M. Leino and R. Mann, *Eur. Phys. J. A* **22** (2004) 417.
- [34] Yu.Ts. Oganessian, *Yad. Fiz.* **63** (2000) 1391; *Phys. At. Nucl.* **63** (2000) 1315.
- [35] S. Hofmann and G. Münzenberg, *Rev. Mod. Phys.* **72** (2000) 733.
- [36] Yu. Ts. Oganessian *et al.*, *Phys. Rev. C* **69** (2004) 021601(R).
- [37] K. Morita *et al.*, *J. Phys. Soc. Jpn* **73** (2004) 2593.
- [38] S. Hofmann, *Rep. Prog. Phys.* **61** (1998) 639.
- [39] S. Hofmann, *Acta Phys. Pol. B* **30** (1999) 621.
- [40] F. Tondeur, S. Goriely, J.M. Pearson and M. Onsi, *Phys. Rev. C* **62** (2000) 024308.
- [41] I. Muntian, Z. Patyk and A. Sobiczewski, *Acta Phys. Pol. B* **32** (2001) 691.
- [42] S. Liran, A. Marinov and N. Zeldes, *Phys. Rev. C* **62** (2000) 047301.
- [43] W.D. Myers and W.J. Świątecki, *Nucl. Phys. A* **601** (1996) 141.
- [44] P. Möller, J.R. Nix and K.-L. Kratz, *At. Data Nucl. Data Tables* **66** (1997) 131.
- [45] S.G. Kadmenski and W.I. Furman, *Alfa Raspad* (Energoatomizdat, Moscow, 1985) (in Russian).

- [46] R.G. Lovas, R.J. Liotta, A. Insolia, K. Varga and D.S. Delion, *Phys. Rep.* **294** (1998) 265 .
- [47] P. Möller and J.R. Nix, *Nucl. Phys. A* **361** (1981) 117; *At. Data Nucl. Data Tables* **26** (1981) 165.
- [48] P. Möller, J.R. Nix, W.D. Myers and W.J. Świątecki, *At. Data Nucl. Data Tables* **59** (1995) 185.
- [49] H.J. Krappe, J.R. Nix and A.J. Sierk, *Phys. Rev. C* **20** (1979) 992.
- [50] V.M. Strutinsky *Nucl. Phys. A* **95** (1967) 420.
- [51] V.M. Strutinsky *Nucl. Phys. A* **122** (1968) 1.
- [52] N.N. Bogoliubov, *Sov. Phys. JETP* **7** (1958) 41; *Nuovo Cimento* **7** (1958) 794.
- [53] N.N. Bogoliubov, *Usp. Fiz. Nauk.* **67** (1959) 549; *Sov. Phys. Usp.* **2** (1959) 236.
- [54] J.G. Valatin, *Phys. Rev.* **122** (1961) 1012.
- [55] M. Bolsterli, E.O. Fiset, J.R. Nix and J.L. Norton, *Phys. Rev. C* **5** (1972) 1050.
- [56] S. Ćwiok, J. Dudek, W. Nazarewicz, J. Skalski and T. Werner, *Comput. Phys. Commun.* **46** (1987) 379.
- [57] A. Sobiczewski, Z. Patyk, S. Ćwiok and P. Rozmej, *Nucl. Phys. A* **485** (1988) 16.
- [58] R. Smolańczuk and A. Sobiczewski, Proc. XV EPS Conf. on nuclear physics: "Low Energy Nuclear Dynamics", St. Petersburg (Russia) 1995, ed. by Yu. Ts. Oganessian, W. von Oertzen and R. Kalpakchieva (World Scientific, Singapore, 1995) p. 313.
- [59] I. Muntian and A. Sobiczewski, *Acta Phys. Pol. B* **32** (2001) 629.
- [60] I. Muntian, Z. Patyk and A. Sobiczewski, *Yad. Fiz.* **66** (2003) 1051; *Phys. At. Nucl.* **66** (2003) 1015.
- [61] I. Muntian, S. Hofmann, Z. Patyk and A. Sobiczewski, *Acta Phys. Pol. B* **34** (2003) 2073.

- [62] A. Türler *et al.*, *Eur. Phys. J. A* **17** (2003) 505.
- [63] Yu.Ts. Oganessian *et al.*, *Nucl. Phys. A* **685** (2001) 17.
- [64] K. Morita *et al.*, *J. Phys. Soc. Jpn.* **73** (2004) 2593.
- [65] G. Audi, O. Bersillon, J. Blachot and A.H. Wapstra, *Nucl. Phys.* **729** (2003) 3.
- [66] A.H. Wapstra, G. Audi and C. Thibault, *Nucl. Phys.* **729** (2003) 129.
- [67] V.E. Viola, Jr., and G.T. Seaborg, *J. Inorg. Nucl. Chem.* **28** (1966) 741.
- [68] A. Sobiczewski, Z. Patyk and S. Ówiok, *Phys. Lett. B* **224** (1989) 1.
- [69] G.A. Lalazissis, M.M. Sharma, P. Ring and Y.K. Gambhir, *Nucl. Phys. A* **608** (1966) 202.
- [70] W. Zhang, J. Meng, S.Q. Zhang, L.S. Geng and H. Toki, *Nucl. Phys. A* **753** (2005) 106.
- [71] A. Parkhomenko and A. Sobiczewski, *Acta Phys. Pol. B* **36** (2005) 3095.
- [72] I. Ahmad, M.P. Carpenter, R.R. Chasman, J.P. Greene, R.V.F. Janssens, T.L. Khoo, F.G. Kondev, T. Lauritsen, C.J. Lister, P. Reiter, D. Seweryniak, A. Sonzogni, J. Uusitalo, I. Wiederhöver and P. Bhattacharyya, *Phys. Rev. C* **62** (2002) 064302.
- [73] I. Ahmad, F.G. Kondev, E.F. Moore, M.P. Carpenter, R.R. Chasman, J.P. Greene, R.V.F. Janssens, T. Lauritsen, C.J. Lister, D. Seweryniak, R.W. Hoff, J.E. Evans, R.W. Loughheed, C.E. Porter and L.K. Felker, *Argonne National Lab. Reaport: PHY-11069-HI-05* (2005).
- [74] F.P. Hessberger, S. Antalic, B. Streicher, S. Hofmann, D. Ackermann, B. Kindler, I. Kojouharov, P. Kuusiniemi, M. Leino, B. Lommel, R. Mann, K. Nishio, S. Saro and B. Sulignano, *Eur. Phys. J. A* to be submitted (2005).
- [75] R.R. Chasman, I. Ahmad, A.M. Friedman and J.R. Erskine, *Rev. Mod. Phys.* **49** (1977) 833.

- [76] S. Ówiok, S. Hofmann and W. Nazarewicz, *Nucl. Phys. A* **573** (1994) 356.
- [77] S. Ówiok, W. Nazarewicz and P.H. Heenen, *Phys. Rev. Lett.* **83** (1999) 1108.
- [78] Y. K. Gambhir, A. Bhagwat and M Gupta, *Phys. Rev. C* **71** (2005) 037301.
- [79] A. Parkhomenko and A. Sobiczewski, *Acta Phys. Pol. B* **36** (2005) 3115.
- [80] Y.K. Gambhir, A. Bhagwat, M. Gupta and A.K. Jain, *Phys. Rev. C* **68** (2003) 044316.
- [81] P. Ring, *Prog. Part. Nucl. Phys.* **37** (1996) 193.
- [82] K. Rutz, M. Bender, P.-G. Reinhard, J.A. Maruhn and W. Greiner, *Nucl. Phys. A* **634** (1998) 67.
- [83] A.V. Afanasjev, T.L. Khoo, S. Frauendorf, G.A. Lalazissis and I. Ahmad, *Phys. Rev. C* **67** (2003) 024309.
- [84] R.B. Firestone, Table of Isotopes, vol. 2, 8th ed. (J. Wiley, New York, 1999).
- [85] O. Parkhomenko and A. Sobiczewski, *Acta Phys. Pol. B* **35** (2004) 2447.
- [86] I. Ragnarsson, A. Sobiczewski, R.K. Sheline, S.E. Larsson and B. Nerlo-Pomorska, *Nucl. Phys. A* **233** (1974) 329.
- [87] A. Parkhomenko and A. Sobiczewski, *Int J. of Mod. Phys E* **14** (2005) 421.
- [88] A. Parkhomenko and A. Sobiczewski, *Acta Phys. Pol. B* **36** (2005) 3095.
- [89] J.O. Rasmussen, *in Alpha-, Beta- and Gamma-Ray Spectroscopy*, vol. 1, ed. K. Siegbahn (North-Holland, Amsterdam, 1979) p. 701.
- [90] S. Hofmann, *et al. Z. Phys. A* **350** (1995) 277.